NUMERICAL INVESTIGATION OF NON-TRADITIONAL GASEOUS FUEL INJECTION INTO THE IRONMAKING BLAST FURNACE

by

Samuel E. Nielson

A Thesis

Submitted to the Faculty of Purdue University

In Partial Fulfillment of the Requirements for the degree of

Master of Science in Mechanical Engineering

Department of Mechanical and Civil Engineering

Hammond, Indiana

August 2021

THE PURDUE UNIVERSITY GRADUATE SCHOOL
STATEMENT OF COMMITTEE APPROVAL

Dr. Chenn Zhou, Chair

Department of Mechanical and Civil Engineering

Dr. Harvey Abramowitz

Department of Mechanical and Civil Engineering

Dr. Ran Zhou

Department of Mechanical and Civil Engineering

Approved by:

Dr. Xiuling Wang

ACKNOWLEDGMENTS

During the course of writing this thesis I have received significant assistance and support.

I would like to thank the SMSVC for their technical and financial support of this research, as well as Stelco and Linde for their valuable technical contributions, and insights into their industrial processes.

I would like to thank my advisor Dr. Chen Zhou for the opportunity and support in carrying out this work, and my supervisor Dr. Tyamo Okosun for his technical expertise and assistance understanding the physics of the blast furnace, and the process of computational fluid dynamics.

Additionally I would like to thank my advisors Dr. Harvey Abramowitz and Dr. Ran Zhou for their guidance through my studies, and assistance in completing this thesis.

I would also like to acknowledge the technical knowledge and advice I received from the members of the Project Technical Committee for the blast furnace project from the SMSVC, specifically Dr. Stuart Street, for his advice and interest in the project, and his wealth of knowledge on the blast furnace process, John D'Alessio and Shamik Ray, for their insight into the operation of the LEW furnace, and Dr. Megha Jampani for her knowledge, collaboration, and interest with the syngas injection modeling.

I would like to thank the entire Mechanical Engineering Department at Purdue Northwest, and the Staff and Students of CIVS for their support, encouragement, and knowledge.

I would also like to acknowledge that portions of this research have been previously published in the proceedings of AIST and the MDPI Processes Journal.

Lastly I would like to thank my mother, Lorna, for her continuous love and support, and for instilling a steadfast commitment to learning, and an appreciation for the Wonder in the world.

TABLE OF CONTENTS

LIST OF TABLES

LIST OF FIGURES

GLOSSARY

Auxiliary fuel – any additional fuel provided to the furnace other than coke

Bored lance – a lance with additional holes drilled perpendicular to axis of pipe to improve mixing

Burden – the layers of fluxed ore pellets, and coke that are charged into the furnace from the top, and eventually descend to be reduced (in the case of the ore pellets), or to be burned in the raceway (coke)

COG – coke oven gas, a waste product from coke manufacture that can be repurposed as a fuel

Cohesive zone – also termed CZ, is the region of furnace where ore pellets start to coalesce stick together reducing permeability, and where the iron ore ultimately melts

Coke – a refined form of coal used to provide carbon to the BF, and to support the iron ore in the burden, and improve permeability

FT-A – flame temperature analog, a CFD calculated equivalent for RAFT

GHG - greenhouse gases, typically in the form of CO_2

Hot metal – sometimes called HM, is the molten iron that collects in the hearth and is tapped from the furnace

Lance – steel pipe of varying designs used to inject aux. fuel

PH – preheat

Raceway – a quasi-steady state void that forms at top of tuyeres

RAFT – raceway adiabatic flame temperature, temperature of reducing gas

Straight lance – an unmodified lance with no additional holes

Syngas - synthetic gas, manufactured fuel gas, usually some mix of H_2 and CO, with other species depending on specifics

TGT – top gas temperature, temperature of waste gas at top of BF, must be maintained above 100 °C to prevent condensation from forming

Tuyere – a water cooled nozzle used to inject hot blast and auxiliary fuel at near bottom of blast furnace

NOMENCLATURE

A	Preexponential factor
$C_{1\varepsilon}, C_{2\varepsilon}$	Model constants
$C_R, C_R{}'$	Model constants
E_A	Activation energy
ε	Turbulence dissipation rate
Γ_i	Species diffusion coefficient
k	Turbulent kinetic energy
μ_t	Turbulent viscosity
R	Universal gas constant
ρ	Density
R_i	Net species production rate
$\sigma_k, \sigma_\varepsilon$	Model constants
s	Specific oxidizer rate
S_i	Species source term
S_{ij}	Strain rate tensor
T	Temperature
$\boldsymbol{U}$	Velocity vector
Y_i	Species mass fraction

ABSTRACT

As the largest source of iron in North America, and as the largest energy consumer in the modern integrated steel mill, the blast furnace is a critical part of modern ironmaking. Any improvements that can be made to the efficiency or emissions of the blast furnace can have far reaching environmental impacts as the production of one ton of steel results in 1.85 tons of carbon dioxide emissions. Given the concerted push to reduce greenhouse emissions, novel technologies are needed to improve efficiency. In this study the injection of preheated natural gas, precombusted syngas from a variety of feedstocks, and hydrogen injection were all modeled using computational fluid dynamics, from the tuyere through the shaft of the furnace. The impacts of these various operational changes were evaluated using CFD calculated analogs for Raceway adiabatic flame temperature (RAFT), top gas temperature (TGT), and coke rate (CR). Results indicate that a reduction of 3% to 12% in CO_2 emissions is possible through the implementation of these technologies, with each possessing distinct benefits and drawbacks for industrial implementation.

1. INTRODUCTION

The ironmaking blast furnace (BF) is responsible for 73% of hot metal production in North America and represents the largest consumer of energy in the entire mill [1]. Given the scale of the operation, minor improvements to the efficiency of the BF can result in significant reductions in operating expenses and carbon emissions. The BF is a counter-current packed bed chemical reactor, where fluxed iron ore pellets and coke lumps are charged into the top of the furnace in alternating layers, with heated air known as hot blast (HB) and any auxiliary fuels such as natural gas (NG) or pulverized coal is injected into the furnace through ports known as tuyeres. The hot blast forms a void space in the coke bed surrounding the tuyeres known as the raceway through the combination of HB gas momentum displacing coke and coke consumption in reactions with HB-supplied oxygen. Although the raceway is constantly changing it approaches a semi-steady state shape.

One of the earliest techniques developed to reduce the amount of coke needed to process iron ore was the introduction of hot blast. Heating the blast supplies additional sensible heat to the furnace to fuel reduction reactions, decreasing the need for coke combustion to supply energy. Later developments included the introduction of auxiliary fuels injected through the tuyeres, supplementing the reducing gas generated by coke combustion with alternative forms of carbon and hydrogen. This alternate supply of reducing gases can reduce the amount of coke required to smelt the iron ore, however it also influences BF operation in key ways, including by altering the reaction kinetics in the shaft region. The introduction of hydrogen gas in addition to carbon monoxide, for instance, can improve productivity in the furnace [2].

In North America NG injection has seen wide adoption due the low fuel cost and ease of handling compared with pulverized coal injection (PCI). This has the benefit of increasing the amount of hydrogen in the BF, thus reducing the overall emissions of CO_2 when compared against a PCI or coke only furnace. One significant limitation to the injection of NG is the quenching effect that it has on gas temperatures in the raceway. For a furnace operating at high natural gas injection rates, the limited gas residence time in the raceway can result in the inability to combust all injected NG. This un-combusted fuel then enters the coke bed and decomposes into carbon and hydrogen in the high temperature, low oxygen environment, further quenching gas temperatures, due to the endothermic nature of the reaction. Any CO_2, or H_2O that forms from NG combustion

will also undergo endothermic decomposition reactions once it enters the coke bed. These reactions however tend to have less of an impact on RAFT, due to the heat released during combustion that resulted in their formation [6].

Industry uses the Raceway Adiabatic Flame Temperature (RAFT) to quantify the available heat in the BF. The RAFT is the calculated value, based on simple energy conservation that measures the temperature of the bosh gas in the furnace once it has been converted to only CO, H_2, and N_2. Natural gas injection will lower the RAFT value, at extremely high injection rates can lower temperatures inside the furnace enough that stability may become an issue. This quenching is typically countered by increasing the oxygen enrichment in the hot blast to raise the RAFT again [3]. This, however, presents its own set of issues, as increasing oxygen enrichment lowers the top gas temperature (TGT). The top gas temperature is the temperature of the waste gas that exits the top of the furnace. Its temperature must be maintained above 100°C to prevent condensation from forming in the upper parts of the furnace. It is this interplay between NG injection lowering the RAFT and raising the TGT, combined with oxygen enrichment that raises RAFT and lowers TGT, which defines the limits of the operating window.

Devising new methods to expand the operating window could provide blast furnace operators with a wider range of operating conditions, potentially reducing operating costs, and emissions. One of the most common existing methods used to expand the operating window is to increase the supply of sensible heat to the furnace, usually in the form of increasing hot blast temperature (HBT). However, many industrial furnaces are already operating at their maximum possible HBT with their existing hot stove designs.

One potential method of increasing the sensible heat entering the furnace is to preheat the natural gas prior to injection. This would have the additional benefit of decreasing the density of the natural gas, resulting in higher injection velocities, which would in turn lead to improved mixing and combustion, and potentially improved heat release [4-6]. This approach was described in limited detail by Feshchenko, in these two papers published between 2007 and 2008, based on two Russian blast furnaces The a papers describe a small heat exchanger that attaches to the elbow of the blowpipe and was able to realize a 200°C natural gas temperature, with the coke replacement ratio shifting from 1.2:1 in the baseline to 1.42:1 with preheating [4,5]. This increase in sensible heat would expand the operating window and potentially allow additional natural gas injection while maintaining reasonable temperatures in the furnace. The increased natural gas injection

would also increase the amount of hydrogen in the furnace, shifting away from CO as the reducing gas, and reducing carbon emissions.

A theoretical limit on the feasibility of natural gas preheating is reached at an injection temperature of approximately 900K, due to the likelihood of inducing gas cracking and the subsequent deposition of carbon in the heat exchangers and supply lines [7]. One potential method to overcome this is to pre-combust the natural gas, or other potential feedstock gases, to create syngas. This resulting hot mixture (consisting primarily of CO and H_2) can then be injected into the BF. Syngas injection also serves to address the issue of low residence time in the raceway, as a syngas generation reactor would allow for sufficient residence time to allow the near complete combustion of the feedstock. Syngas injection would adjust the balance of H_2 to carbon in the bosh gas by expanding the operating window and allowing increased amounts of auxiliary fuel to be injected while maintaining sufficiently high temperatures While syngas injection still introduces additional carbon to the furnace, it represents a more moderate step that may be easier to control and implement for standard blast furnace operations which currently utilize NG as an injected fuel.

Given the increasing prevalence of carbon taxes worldwide, and additional regulations on carbon emission which may be imposed in attempts to control climate change, there is growing industrial interest in the injection of hydrogen-rich fuels into the BF. Typically, in a modern BF, hydrogen only enters as water vapor in the HB either from ambient humidity, from steam injection, or from the injected fuels. ThyssenKrupp in Germany has already began operating a BF using hydrogen as the injected fuel at a single tuyere to reduce carbon emissions [8]. Hydrogen injection presents a unique challenge as it is a raw reducing gas that provides no heat to the furnace as any combustion reactions in the tuyere are immediately reversed in the high temperature low oxygen environment of the coke bed. Due to this upper end of injection rates are somewhat limited [9]. Hydrogen injection therefore must rely on other means of introducing sensible heat to the furnace. One potential solution is the injection of high temperature hydrogen at the tuyere. This is somewhat similar to the midshaft injection of hot reducing gas that was previously explored by Pistorius et. al. [3]. Because hydrogen is resistant to decomposition at much higher temperatures than methane, preheating could reach significantly higher temperatures, thus providing more heat to the furnace.

Blast furnace modeling and research techniques fall into four broad categories experimentation with full size industrial furnaces, experimentation with small-scale furnaces, heat and mass balance models, and, finally, computational fluid dynamics (CFD). Experimentation with

industrial furnaces is an expensive and potentially dangerous process that can interfere with normal operation of the furnace, and potentially cause periods of decreased productivity. For this reason it is rarely used today. Small-scale experimental furnaces are cheaper than full-scale furnaces, but are still comparably expensive when compared with the two modeling methods. Experimental furnaces also suffer from some issues with scaling results to larger furnaces due to their smaller size, and reduced output. Heat and mass balance models have long been the staple method of BF analysis, as they are computationally simple and can provide insight into the overall thermodynamic behavior of the furnace [10]. These models must make assumptions about the efficiency of certain reactions and certain chemical equilibriums thorough the furnace. Because of this certain data from actual operation is needed to calculate accurate predictions. However with operational furnaces where historic data is available heat and mass balance models are useful for online control due to their speed.

Computational fluid dynamics presents a method of capturing more complicated physics than the simple heat and mass balance models at the cost of increased model complexity, increased computational expense, and increased solution time. This limits the applicability of CFD for online control applications but makes it a valuable tool for investigating potential changes to BF operation that would be prohibitively expensive, or geometry changes that would require significant rebuild efforts [11-19].

2. METHODOLOGY

To limit the number of operating conditions that could be varied, as well as to focus on modern BFs, a natural gas only furnace was chosen for this work. The Stelco Lake Erie Works (LEW) furnace is located on the north shore of Lake Ontario, was constructed in 1980's and is the newest BF in North America. The BF used for modeling is a relatively large blast furnace, which only injects natural gas as an auxiliary fuel. This removes the impact of PCI injection, and allows modeling work to exclusively focus on the impacts of gaseous fuels. Dimensions and general operating conditions are outlined in Table 1, and Figure 1. Baseline operation uses a bored lance for natural gas injection as detailed in Figure 1. This lance is constructed from a standard length of schedule 40 1.25 inch diameter steel pipe. A series of holes are then bored into the end, with an aim to improve the mixing of the hot blast and natural gas, and result in more combustion. Figure 2 provides dimensions and additional views of the bored lance.

Table 1: Stelco LEW operating conditions

Wind Rate	270,000 nm^3/hr (3.86 kg/s per tuyere)
Hot Blast Temperature	1448K (1175 °C, 2147 °F)
O_2 Volume Fraction	29.12%
Blast Moisture	23 grams/nm^3
NG Injection Rate	95 kg/THM, 36,170 nm^3/hr (0.28 kg/s per tuyere)
Baseline NG Temperature	300K
Hot Metal Production	6580 THM/day

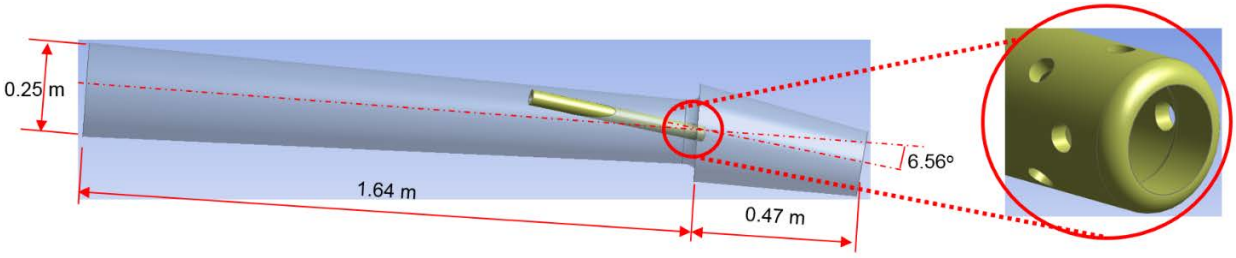

Figure 1: Tuyere and lance geometry, including bored lance detail view

CFD Models

To capture the complexity and varied physics in the blast furnace the furnace was split into three segments to allow modeling to only focus on the relevant physics and phenomenon in each region of the furnace. These three regions cascade from one to the other, with a one-way coupling, to feed data into the next step of the modeling process. The particulars of this modeling approach have been covered in previously published work in far greater detail [22-39]. For the sake of brevity a short overview will be provided here. The three regions that the furnace was discretized into are the tuyere, raceway, and shaft regions. Because of the periodic symmetry of the BF only a single tuyere was modeled. The tuyere and raceway are modeled as a 3D domain to capture the asymmetry of fuel injection lances. By the time the gas reaches the upper levels of the raceway domain gas distributions are largely uniform radially. This allows the shaft region to be modeled as a 2D axisymmetric domain to reduce the computational cost and improve solution times.

To further reduce the computational cost of modeling, several foundational assumptions were made. Firstly, that the time scales of the gas and solid flow in the furnace are sufficiently different, being separated by approximately 4 orders of magnitude, that the solid phase can be assumed fixed, and modeling can focus primarily on the motion of the gas phase. With this approach the solid phase forms a fixed porous bed that is able to participate in chemical reactions, heat transfer, and flow interactions with the surrounding gas phase. Secondly, that the furnace has periodic symmetry, and that all tuyeres receive the same mass and temperature of hot blast, and that major conditions do not vary around the circumference of the furnace.

The final assumption is that the furnace operates at a steady state condition, when stability has been reached. To model coke combustion in the raceway, the porosity distribution in the coke bed is assumed to be fixed, approximating the quasi-steady state shape of the raceway. One artifact of this assumption is that when coke takes part in a chemical reaction and leaves the solid phase for the gas phase, there is no reduction in the amount of coke present in the domain. This is justified based on the large reservoir of coke available above the raceway in the shaft of the furnace. Any small amount that is consumed will be almost immediately replaced by burden above it.

The tuyere region was modeled using the commercial CFD code FLUENT™. This permits rapid design changes to the injection lance geometry and location, allowing investigations of combustion and heat transfer in the tuyere region without needing to capture the full complexity of the furnace. This is beneficial for small scale design studies, and allows for simplified case setup

when running large case matrices. In the tuyere region the primary concern is capturing the turbulent mixing of the hot blast and any auxiliary fuel plumes, and the resulting combustion reactions.

This is accomplished using the standard Navier-Stokes equations with the Semi-Implicit Method for Pressure Linked Equations (SIMPLE) scheme for pressure coupling. The Discrete Ordinates Model was used to account for radiation heat transfer from the high temperature raceway.

The k-ε turbulence model used to address the effects of turbulence. As a two equation model it adds minimal computational cost, while capturing the effects of turbulent mixing. This model accomplishes this by modeling the transport of turbulent kinetic energy with Equation 1, and the rate of turbulent dissipation with Equation 2.

$$\nabla \cdot (\rho k \boldsymbol{U}) = \nabla \cdot \left(\frac{\mu_t}{\sigma_k} \nabla \mathrm{k}\right) + 2\mu_t S_{ij}.S_{ij} - \rho\varepsilon \tag{1}$$

Where ρ is the density, k is the turbulent kinetic energy, **U** is the velocity vector, μ_t is the turbulent viscosity, σ_k is a model constant equal to 1.00, S_{ij} is the strain rate tensor, and ε is the turbulence dissipation rate.

$$\nabla \cdot (\rho \varepsilon \boldsymbol{U}) = \nabla \cdot \left(\frac{\mu_t}{\sigma_\varepsilon} \nabla \varepsilon\right) + C_{1\varepsilon} \frac{\varepsilon}{k} 2\mu_t S_{ij}.S_{ij} - C_{2\varepsilon} \rho \frac{\varepsilon^2}{k} \tag{2}$$

Where ρ is the density, ε is the turbulence dissipation rate, **U** is the velocity vector, μ_t is the turbulent viscosity, σ_k is a model constant, S_{ij} is the strain rate tensor, σ_ε is a model constant, and finally $C_{1\varepsilon}$ and $C_{2\varepsilon}$ are both model constants, valued at 1.44 and 1.92 respectively.

The Species Transport Model with the Eddy Dissipation Concept model and a two-step methane combustion mechanism to model reactions and mixing, with additional reactions to track methane decomposition and hydrogen combustion. The general species transport equation is detailed in Equation 3:

$$\nabla \cdot (\rho \mathbf{U} Y_i) = \nabla \cdot (\rho \Gamma_i \nabla Y_i) + R_i + S_i \tag{3}$$

Where ρ is the density, and ε is the turbulence dissipation rate, **U** is the velocity vector, Y_i is the mass fraction of a given species, Γ_i is the species diffusion coefficient, R_i is the net production rate of that species via chemical reactions, and S_i is the rate of creation of that species from all other sources, this is applied to manage the impact of mass transfer from solid combustion in subsequent regions of the furnace.

The raceway region is modeled using a combined approach which applies both existing in-house CFD code and commercial CFD code. This model makes use of a two-step process to model the formation and subsequent combustion in the raceway. The first step is to use a transient interpenetrating two-phase Eulerian-Eulerian multiphase model in the commercial CFD code FLUENT™ to perform a cold flow simulation which provides a prediction of the size and shape of the raceway cavity. The flow time for the final raceway shape result varies depending on operating conditions, with the selection point defined as the latest timestep in which the raceway cavity in the fluidized coke bed remains attached to the tuyere nose.

The coke phase distribution is then exported and used in the in-house code to provide a fixed porosity distribution that defines the raceway. Reactions in this region are modeled using a combination of the Eddy Breakup Model and a simple Arrhenius rate model, with the lowest rate of reaction between the two being used as the limiting reaction rate in the model. Equation 4 depicts the standard form of the Arrhenius reaction rate:

$$w_{Arr} = A\rho^2 Y_{Fuel} Y_{O2} exp(-\frac{E_A}{RT}) \quad (4)$$

Where A is the pre-exponential factor, ρ is the density , Y_x is the mole fraction of a particular species, E_A is the activation energy, R is the universal gas constant, and T is the gas temperature. The second reaction rate calculated by the model is the EBU based rate:

$$w_{EBU} = -\rho \frac{k}{\varepsilon} \min\left(C_R Y_{Fuel}, C_R \frac{Y_{O2}}{s}, C'_R \frac{Y_{product}}{1+s}\right) \quad (5)$$

Where C_R and $C`_R$ are model constants, and *s* is the specific oxidizer rate. The raceway combustion model then compares the two reaction rates for each cell at each time step, and

utilizes the lowest production rate to calculate the updated cell values. This is to address the two fundamental limiting factors in non-premixed combustion. At low temperatures the reaction rate is primary limited by the available thermal energy, and the speed of the chemistry. As the temperature increases the limiting factor becomes speed with which fuel and oxidizer can be mixed, and the speed of the reaction is governed by local turbulent conditions. This approach prevents reactions from occurring when there is insufficient thermal energy available.

The coke bed is modeled as an infinite amount of carbon in the regions outside the raceway. This approximation is based on the quasi-steady state nature of the raceway. Any particular piece of coke that is consumed in the raceway will soon be replaced by the large reserve of coke in the shaft of the furnace. This, combined with the melting of iron in the CZ, is the principal mechanism of burden consumption and thus drives the descent of the burden. Further details of this raceway model, including additional validation can be found in previously published work [22-27]. Details of the chemical kinetics and reaction rates used in the raceway combustion model can be found in Table 2 below.

Table 2: Key reaction mechanisms and kinetics for the CFD raceway combustion model [32, 31].

Reaction	**A [1/s]**	**Activation Energy, E_A [J/mol]**
$CH_4 + 2O_2 \rightarrow CO_2 + 2H_2O$	7.94×10^{11}	1.081×10^5
$2CO + O_2 \rightarrow 2CO_2$	2.23×10^{12}	6.651×10^4
$2H_2 + O_2 \rightarrow 2H_2O$	9.87×10^8	1.255×10^5
Coal Moisture Evaporation	4.16×10^7	4.228×10^4
Coal Devol. Reaction 1	3.7×10^5	7.366×10^4
Coal Devol. Reaction 2	1.46×10^{13}	2.511×10^5
$C + O_2 \rightarrow CO_2$	1.225×10^3	9.977×10^4
$2C + O_2 \rightarrow 2CO$	1.813×10^3	1.089×10^5
$C + CO_2 \rightarrow 2CO$	7.351×10^3	1.380×10^5
$C + H_2O \rightarrow CO + H_2$	1.650×10^5	1.420×10^5

Using the temperature dependent density distributions and the mass transfer to the gas phase from coke bed, the Eulerian-Eulerian multiphase model is then used with these two new source terms. This effectively includes the impact of increasing gas volume due to coke combustion and the changes in gas momentum as a function of density. A new coke bed porosity distribution is then generated using the same methodology as before, and the resulting porosity distribution is then used to run a new combustion simulation using the in-house code. This process

is repeated once more to reach a final converged raceway shape. Due to the extended run time of the full raceway formation model, and its primary dependence on blast conditions, the decision was made to use the baseline porosity distribution. The resulting gas species, temperature, and velocity distributions are then compressed azimuthally to generate an averaged radial distribution.

The raceway region combustion model is used to calculate a CFD analog to the theoretical RAFT (raceway adiabatic flame temperature) used in industrial operations. This analog termed Flame Temperature Analog (FT-A) is calculated by taking the mass weighted temperature average of all cells in the domain above the centerline of the tuyere with a gas mass fraction below 0.5% for all of the following species: CO_2, O_2, H_2O, and CH_4. This provides a method of comparing the temperature of the bosh gas in the furnace under different scenarios and provides a representation of the available heat in the furnace to reduce iron ore, as well as a touchstone for comparison to existing operational practices that is familiar to the industrial operator.

The shaft region is modeled using in-house FORTRAN code that tracks the motion of the bosh gas, the reduction of the fluxed iron ore pellets contained in the solid phase, the heating of the ore as it approaches the cohesive zone, and various chemical reactions that occur in the shaft region. The chemical kinetics modeled in the shaft region include the 6 ore reduction reactions, the water gas shift reaction, flux decomposition, the Boudouard reaction, and direct reduction of liquid FeO, a summary of these reactions can be found in Table 3.

Table 3: Reaction mechanisms used in the CFD shaft model.

Reaction	**No.**	**Chemical Equation**
Indirect reduction of iron oxide by CO	R1	$3Fe_2O_3(s) + CO(g) \rightarrow 2Fe_3O_4 + CO_2(g)$
	R2	$Fe_3O_4 + CO(g) \rightarrow 3FeO(s) + CO_2(g)$
	R3	$FeO(s) + CO(g) \rightarrow Fe(s) + CO_2(g)$
Indirect reduction of iron oxide by H_2	R4	$3Fe_2O_3(s) + H_2(g) \rightarrow 2Fe_3O_4 + H_2O\ (g)$
	R5	$Fe_3O_4 + H_2(g) \rightarrow 3FeO(s) + H_2O(g)$
	R6	$FeO(s) + H_2(g) \rightarrow Fe(s) + H_2O(g)$
Boudouard reaction	R7	$C(s) + CO_2(g) \rightarrow 2CO(g)$
Water gas reaction	R8	$C(s) + H_2O(g) \rightarrow CO(g) + H_2(g)$
Flux decomposition	R9	$MeCO_3(s) \rightarrow MeO(s) + CO_2(g)$ (Me = Ca, Mg)
Water gas shift reaction	R10	$H_2(g) + CO_2(g) \rightarrow H_2O(g) + CO(g)$
Direct reduction of liquid FeO	R11	$C(s) + FeO(l) \rightarrow Fe(l) + CO(g)$

The location and shape of the cohesive zone (CZ) is calculated by drawing two isotherms based on the temperature of the solid phase. The upper limit of the CZ is defined as the softening temperature of the iron ore, 1473K in this case, and the lower limit is defined by the liquidous temperature of the ore, here 1673K. In the cohesive zone the porosity of the ore layers is assumed to be zero, and all gas flow must pass through the coke slits, that retain their original porosity. Additional details on the specifics of the model and validation work can be found in previously published work [29,31,38,37].

To capture the impact of flux on furnace operation it is assumed that the volume of flux is sufficiently low that it can be modeled as uniformly distributed through the ore layers. This allows for the flux decomposition reactions to be modeled, and the contours of flux species to be tracked.

Natural Gas Preheating Methodology

To evaluate the impact of natural gas preheating in the BF a baseline case was modeled using input data from Stelco. This model was then calibrated to bring results in line with industrial expectations. Nine natural gas injection rates and four preheat levels were selected for simulation. These particular parameters are outline in Table 4, resulting in 36 total cases for this study. The range of injection rates was chosen to explore the range around the baseline 95 kg/THM, including the potential to increase the natural gas injection rate.

The upper limit for NG injection temperature is approximately 900K (673°C), beyond this temperature the risk of CH_4 decomposition increases dramatically, and problems may arise from soot deposition. The decision was made based on conversations with BF operators to limit the upper level of preheating to 600K (327 °C). This is due in part to safety concerns, and then the perceived difficulty of realizing NG injection temperatures above 600K while using waste heat.

To evaluate the efficiency of preheating a preheating efficiency was defined as the ratio of the increase in FT-A to the injectant preheat. This provides a method of comparison between various injectant flow rates and compositions. Given that the impacts of preheating were found to be largely linear this also allows for limited extrapolation beyond the preheating ranges examined here.

Table 4: Natural gas case matrix

NG Rate (kg/THM)	NG Temp
85	25 °C (baseline) (300K)
95 (baseline)	125 °C (325K)
105	225 °C (350K)
110	325 °C (375K)
115	
120	
130	
140	
150	

Syngas & Hydrogen Injection

Syngas is a manufactured mixture of combustible gases, typically containing a mixture of CO and H_2 as the predominant fuel species. Syngas can trace its roots to the town gas of the early 20^{th} century when coal was partially burned to generate town gas. Partial combustion remains one of the most common methods of generating syngas, requiring only a feedstock and oxidizer stream, and the appropriate reactor for the reactions to occur. The outlet temperature and composition of the resulting syngas are a function of the feedstock flowrates and reactor design.

Syngas injection was modeled using the same methodology as NG preheating, with the existing reaction models. The case matrix is outlined in Table 5. Due to the decreased density of the syngas resulting from the higher temperatures and increased free hydrogen content the diameter of the fuel lance was increased to 2 inches vs the original 1.25 inches of the bored lance. This increases the cross-sectional area of the lance and decreases the injection velocity (Figure 2). A lance without boreholes at the end is commonly referred to as a straight lance by the plant operators, and this terminology will also be applied here.

Three potential syngas compositions were provided by Linde based on their existing technologies. These three compositions are outlined in Table 6. These three compositions were selected to investigate different potential feedstocks based on feedback from industrial collaborators. These are a natural gas based syngas, where the feedstock supplied to the reactor for the express purpose of generating syngas. The two remaining compositions both use Coke Oven Gas (COG) as the feedstock for the syngas reactor. Coke oven gas is a byproduct of coke

production, and consists of volatiles and carbon monoxide driven off from the coal as it is cooked to form coke. Because COG is a waste byproduct that can be reused to extract thermal energy COG derived syngases will have a lower total carbon footprint than natural gas derived syngas.

Table 5: Syngas case matrix

Syngas Rate (kg/THM)	Composition	Temperature	Hot blast oxygen
80	NG Feedstock	High temp. 1673-1562K (1400-1289°C)	Constant
85	COG Feedstock #1	973K (700 °C)	Adjusted
90	COG Feedstock #2	673K (400 °C)	
95			
100			
105			
110			
120			
130			
140			
150			

Three temperatures: 673K (400°C), 973K (700°C), and a "high temperature case" were selected for modeling. The high temperature cases are based on the temperature of the syngas at the outlet of the syngas generator, with the other two temperatures representing potential quenching and heat losses in the supply piping. This resulted in a total of 55 syngas cases.

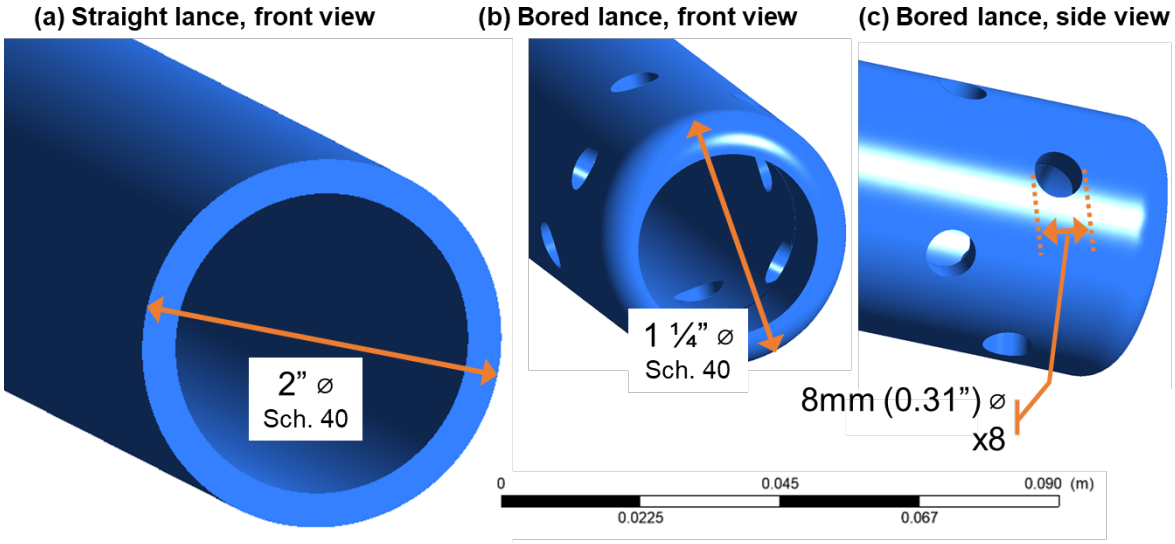

Figure 2: Comparison of straight-pipe lance (a) and bored lance (b&c) geometry

Table 6: Syngas compositions

Parameter	NG Feedstock	COG Feedstock #1	COG Feedstock #2
Gas Temp.	1673K (1,400°C, 2,547°F)	1562K (1,289°C, 2,350°F)	583K (310°C, 590°F)
CO Vol%	31.9%	20.9%	18.1%
CO_2 Vol%	1.9%	2.2%	2.7%
H_2 Vol%	54.9%	52.9%	52.2%
H_2O Vol%	10.6%	16.0%	10.8%
CH_4 Vol%	0.5%	3.0%	11.4%
Effective HB O_2	30.1%	31.52%	31.53%

Hydrogen injection was also modeled using the same methodology as NG injection. Similar to the syngas injection cases the larger diameter straight lance was used to reduce the injection velocity and minimize impingement on the tuyere wall. Due to hydrogen's significantly lower density compared to NG comparisons on the basis of mass based injection (kg/THM) are of limited utility. Molar flow rates allow for a more consistent method of comparing axillary fuel injection. See Figure 3 for more detail. Reducing gas composition at the bosh is based tuyere level conditions. The CO content is governed by the amount of oxygen and water vapor in the hot blast stream, and the amount of hydrogen is governed by hydrogen content in any injected fuel and the blast moisture. The carbon in the CO at the bosh is from coke that was consumed in the raceway, or carbon in injected fuel.

Given a constant supply of oxygen in the hot blast coke consumption in the raceway will increase as the amount of carbon in the auxiliary fuel decreases. To counter this a series of hydrogen cases were conducted with reduced oxygen. The amount of oxygen removed from the hot blast was calculated to correspond to the theoretical amount of oxygen that would react with the carbon from the NG in the baseline case.

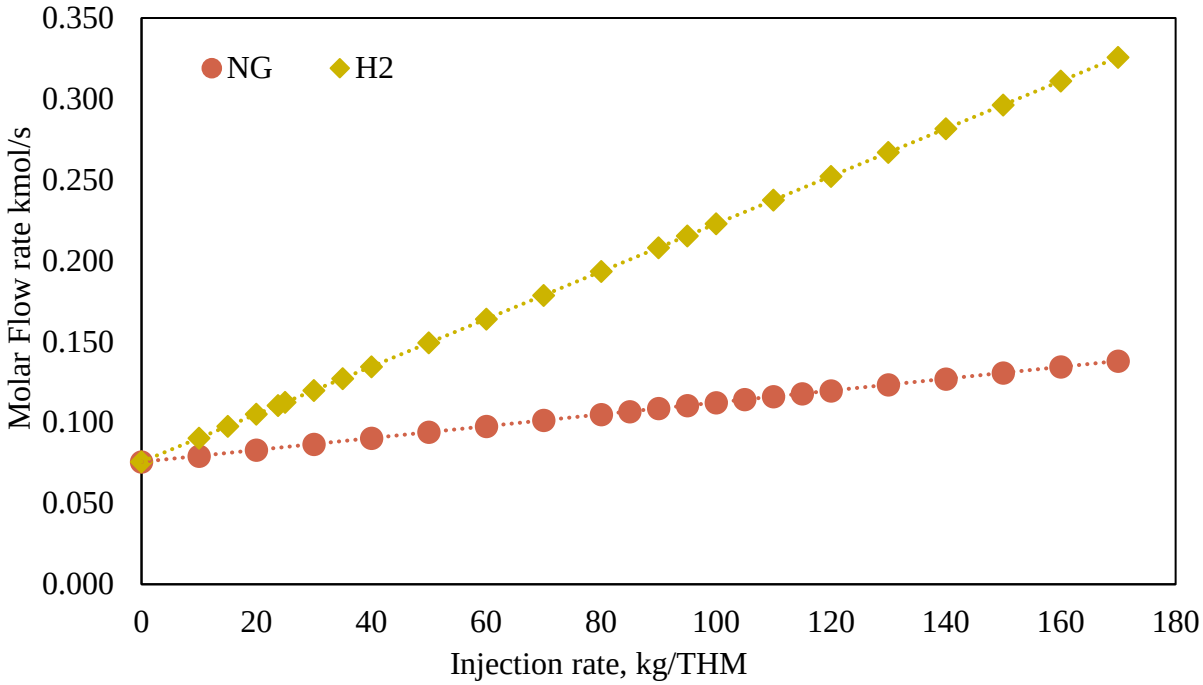

Figure 3: Hydrogen and NG equivalent molar injection rates

3. BASELINE OPERATION RESULTS

Current operating conditions at the Stelco LEW were modeled initially to obtain a validated baseline case. This simultaneously provided validation of the models against the physical furnace, and also created a benchmark that future cases could be compared against to gauge their impact on the furnace. Figure 4 depicts the positioning of the high temperature plume of combustion products from the natural gas in the baseline tuyere case. Here the migration of the high temperature plume is apparent. As the flow moves through the tuyere, the plume moves further and further towards the left hand side of the tuyere (as viewed from outside the furnace). This is a result of the injection lance entering from the right hand side, and imparting a leftward momentum to the auxiliary fuel stream. This is generally not a concern, however when the plume momentum is sufficient to carry the high temperature region into contact with the wall thermal ablation and damage can occur on the tuyere, potentially shortening tuyere life. The particular angle that the injection lance enters the blowpipe at is limited by surrounding equipment on the tuyere deck of the furnace, and would be very difficult and expensive to adjust.

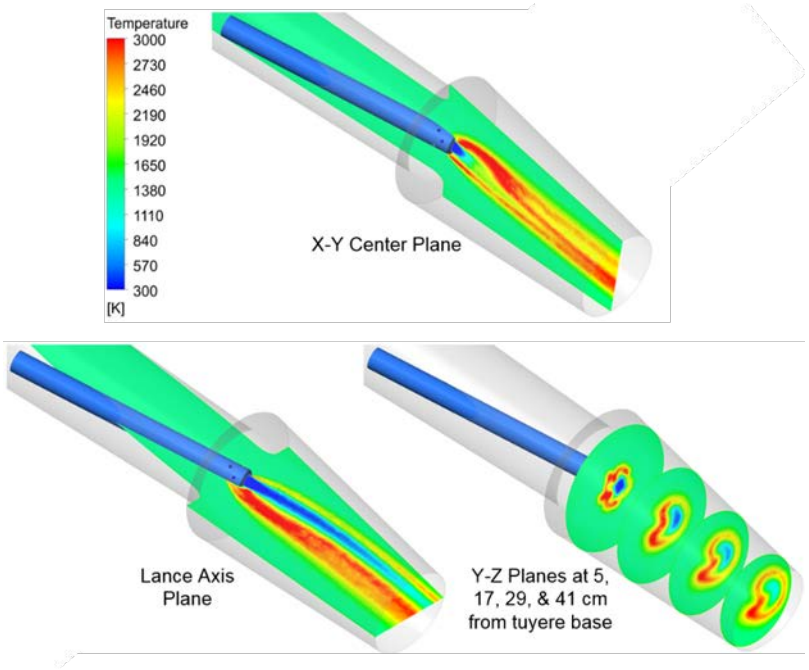

Figure 4: Baseline tuyere gas temperature distributions

Moving to the raceway region asymmetry in the top view contours is readily apparent, the left hand side (LHS) of the raceway, rendered here as the upper half of the top view, is significantly colder than the right hand side (RHS) of the raceway. This is again a result of the lance angle, as the leftward momentum of the plume concentrates uncombusted NG and any products of combustion from the NG on the LHS of the raceway. Once this plume of hot burned and partially burned gases enters the coke bed it undergoes endothermic decomposition reactions, converting everything except nitrogen from the hot blast to CO or H_2. The flame temperature analog (FT-A) for the baseline was found to be 2,182K. This compares very favorably with the industrial heat and mass balance model's calculated value of 2,170K, for a total difference of 0.55%.

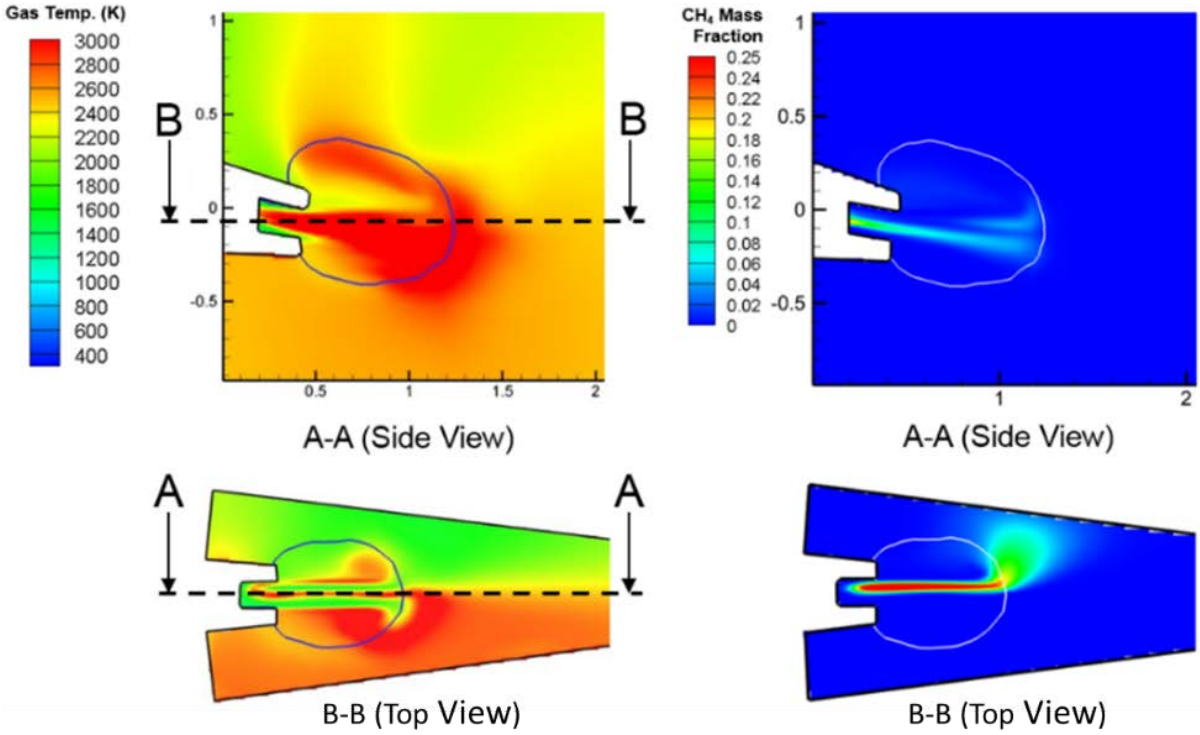

Figure 5: Baseline raceway gas distributions, gas temperature (left), CH_4 mass fraction (right),

Moving to the shaft region the location of cohesive zone as well as the distributions of the major constituent species in the gas phase are presented in Figure 6. Here the shift from CO to CO_2 and from H_2 to H_2O can be observed as the gas rises in the furnace. Table 7 provides an overview of the shaft results and a comparison to the expected values from the plant operators.

Table 7: Baseline validation

	CFD Prediction	Industry Expected Values
Coke Rate	392 kg/THM	~390 kg/THM
CO Utilization	50.77%	~ 50%
H_2 Utilization	51.46%	~ 50%
Avg. Top Gas Temperature	116.46 °C	100 – 110 °C
ΔP (Model bottom to top)	123 kPa	*N/A*

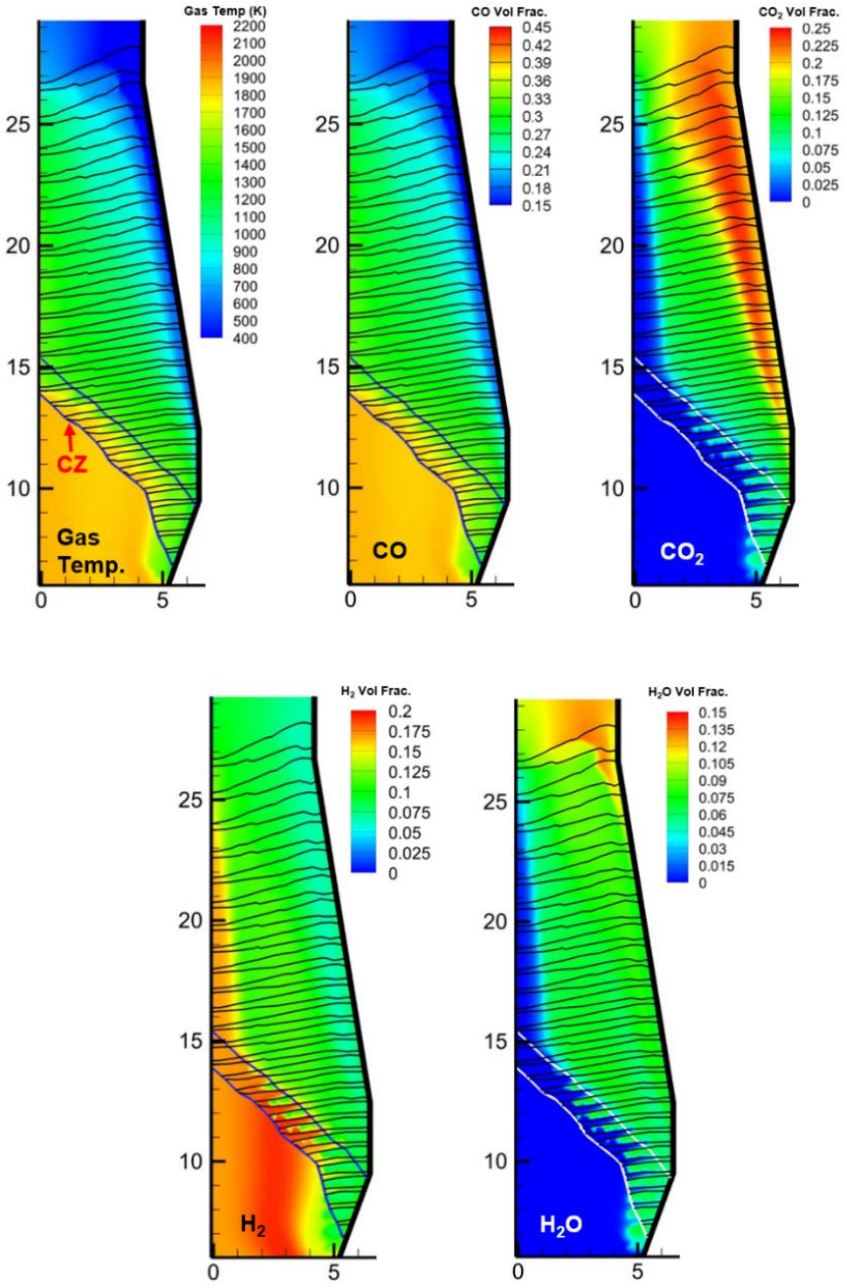

Figure 6: Shaft region contours of gas temperature (top left), CO vol. fraction (top center), CO_2 vol. fraction (top right), H_2 vol. fraction (bottom left), and H_2O vol. fraction for baseline case.

4. NATURAL GAS PREHEATING RESULTS

Initial preheating modeling focused on holding all other operating conditions constant and only adjusting the temperature of the injected natural gas, with preheats of 100-300 Kelvin. The overall gas distributions are similar to the baseline both in the tuyere and the raceway regions, although with minor shifts in the location and size of the high temperature regions. Comparing the 300 K NG preheat to the baseline case, average gas temperature at the tuyere outlet is 1.4% higher and the average gas velocity is 1.8% higher. Gas temperature distributions in the tuyere region for the two extreme cases (baseline and 300K PH) are detailed in Figure 7. The slight shifting of the high temperature region of the NG plume is notable as

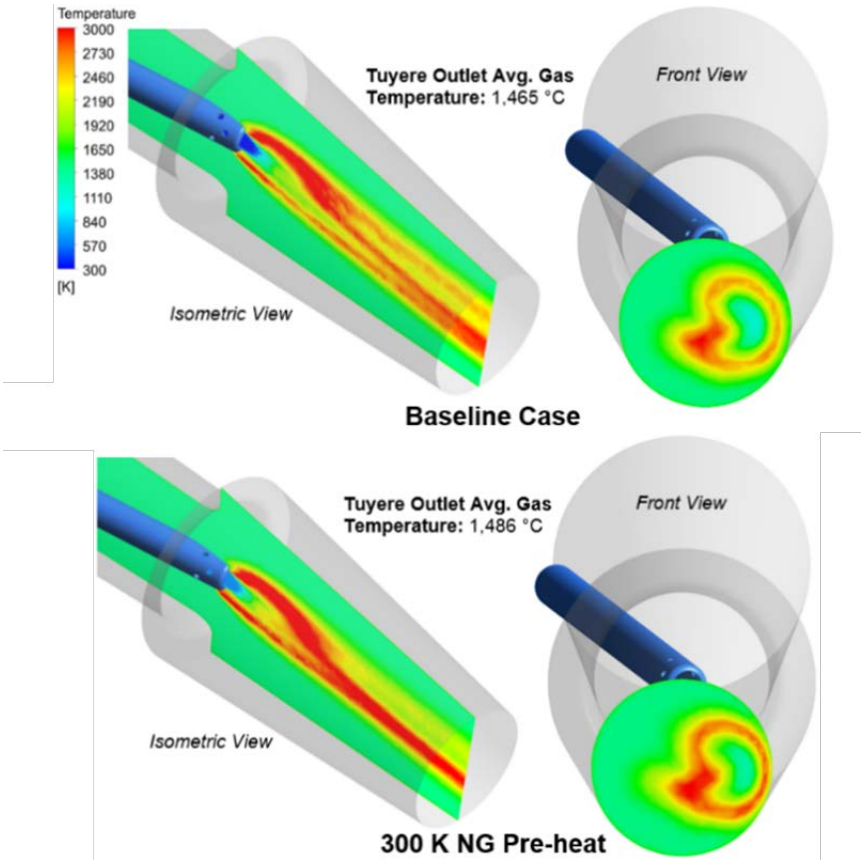

Figure 7: Contours of gas temperature in the tuyere region on a center plane and the tuyere outlet plane for the baseline 0K preheat case (top) and 300K preheat (bottom).

Due to the low residence time in the tuyere, the primary impacts of preheating become apparent in the raceway region. There is minor variation in the distribution of the species and gas temperatures in the raceway between the preheating cases, with the most notable impact being the relatively small increase in FT-A, see Table 8 for details.

Table 8: Preheating impact 95 kg/THM

NG Preheat, K	FT-A, K	Increase from Baseline	
0	2187	-	-
100	2207	20K	0.9%
200	2222	35K	1.6%
300	2239	52K	2.4%

Preheating the injected NG to 300K above ambient resulted in a coke rate reduction of 7 kg/THM and decreased the predicted top gas temperature by 13K relative to the baseline. Shaft results for the 95 kg/THM set of cases are outlined in Table 9. There is a weak trend of increasing gas utilization as the level of preheating increases, likely as a result of the increased reactivity due to higher bosh gas temperatures.

As the level of preheating increases, a downward trend is observed for both the top temperature and the coke rate. This behavior is in line with the impacts of higher bosh gas temperatures (whether they result from increased blast temperature or the NG preheating implemented in this scenario), as documented in numerous industrial rules-of-thumb [2]. This apparent inverse relationship between the FT-A and the top gas temperature is discussed in additional detail in a later section.

Table 9: 95 kg/THM shaft results

Case	CO Utilization	H_2 Utilization	Top Gas Temperature °C	Coke Rate, kg/THM
0K	51.8%	52.2%	130	392
100K	52.2%	52.3%	126	389
200K	52.6%	52.4%	120	387
300K	52.9%	52.5%	117	385

Figure 8 provides an overview of the relatively minor changes in the temperatures and species distributions between the baseline and the 300K preheat (PH) case in the shaft region. As the level of NG preheating increases, the cohesive zone tip shifts downward slightly, while the

predicted root location remains anchored in a similar location on the furnace wall. Additionally, gas species distributions remain almost identical between cases, similar to the gas temperatures.

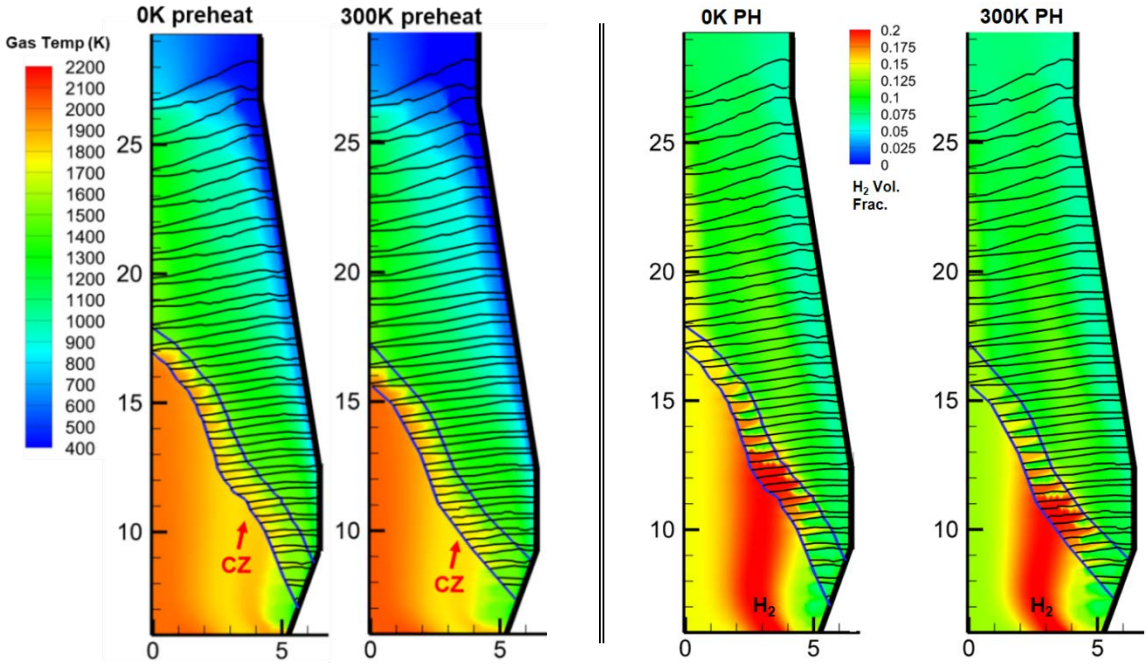

Figure 8: Gas temperature (left) and H_2 %vol. (right) distributions, baseline 0K preheat vs. 300K preheat

Given the impact of NG preheating at a fixed NG injection rate, nine NG injection rates (85 kg/THM to 150 kg/THM) were selected as the primary scenarios to investigate the impact of preheating with variable injection rates, and four different levels of preheating (ranging from 0K to 300K). This range of injection rates was selected to capture the current operating range of a typical North American BF, with the high upper end of injection rates selected to explore the potential to expand the typical window of stable operation to higher injection rates. The Ore/Coke ratio in the burden was adjusted based on industrial practices to account for the increased NG rate. As the injection rate of natural gas increases the O/C ratio in the burden will be shifted towards ore.

One impact of NG preheating that is observed to great effect in the tuyere region is the thermal expansion of gas and corresponding increase in injection velocity. Figure 9 compares the in-lance velocity of the NG versus the injection rate. Gas velocity increases more rapidly with preheating implemented, as the corresponding density of the injected NG falls with increasing

temperature. This increased velocity would lead to increased turbulent mixing between the fuel plume and the hot blast, potentially improving combustion. While the scenarios in this segment of the research all retained the same tuyere/blowpipe/lance geometry, implementation of high-rate NG injection with preheating would likely require larger diameter injection lances to reduce this in-lance velocity at the upper end of injection rates.

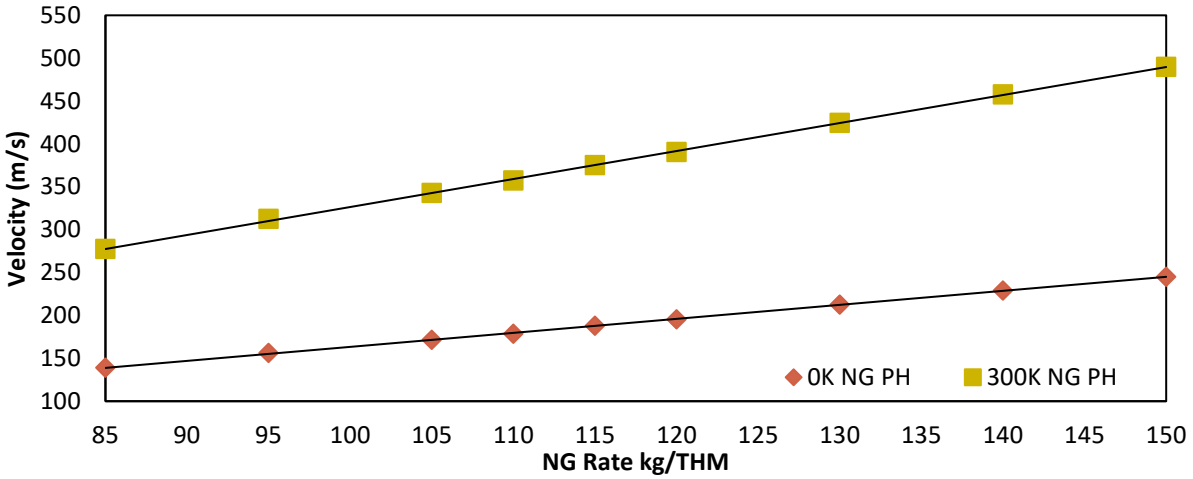

Figure 9: NG lance inlet velocity

The FT-A increases with the amount of preheating for all injection rates, except the 150 kg/THM case. The phenomena responsible for the reduction in effectiveness of preheating at higher injection rates are likely two-fold. First, as the injection rate of NG is increased, the residence time within the raceway falls. Once the NG plume enters the coke bed any remaining NG will crack, consuming heat and lowering gas temperatures. Second, increased NG temperatures will lead to more rapid cracking of any NG that cannot directly combust with O_2, leading to further potential temperature reductions.

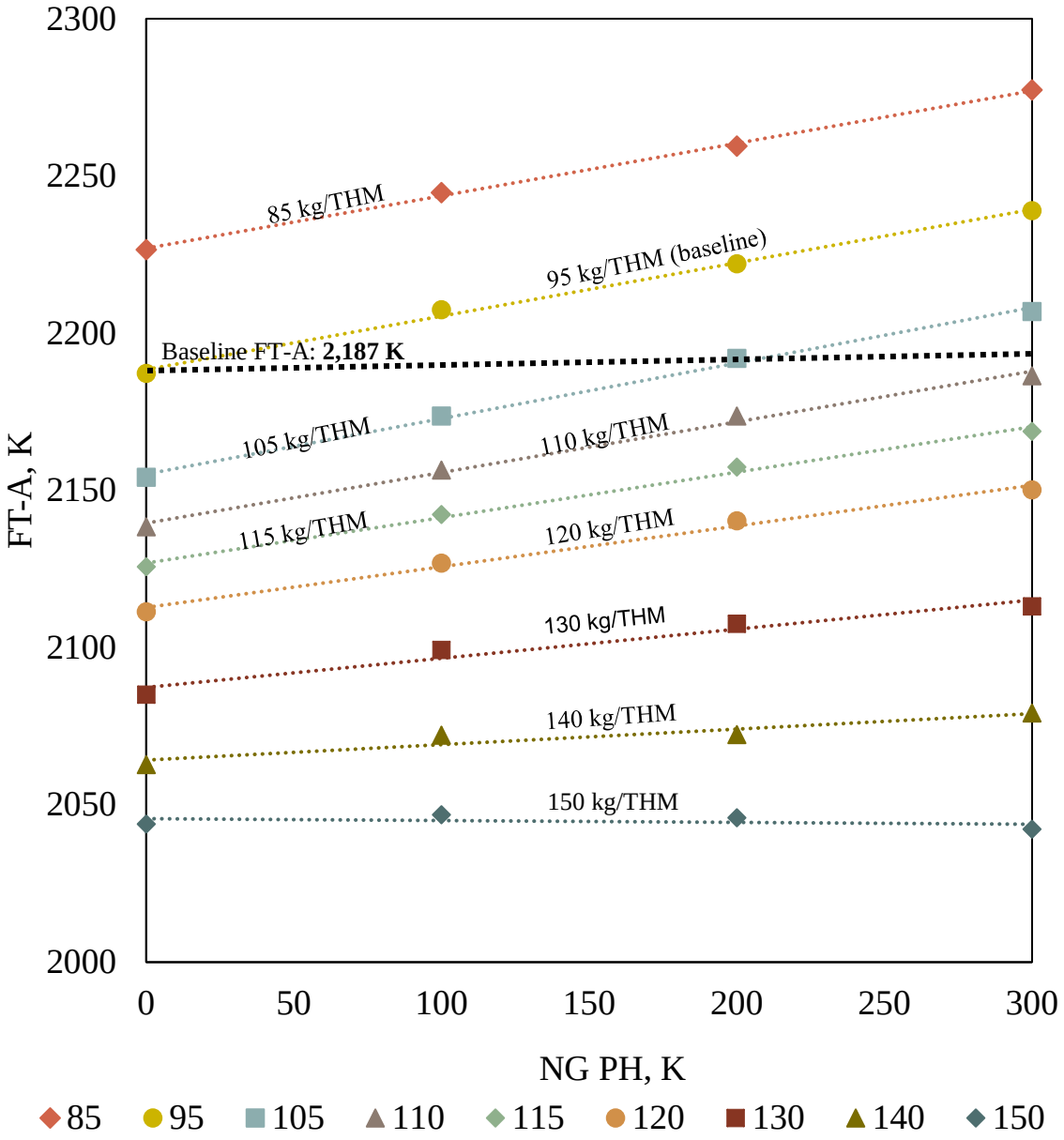

Figure 10: FT-A vs NG preheat across range of injection rates

The slope of the FT-A vs NG preheat trendlines plotted in Figure 10 can be used to describe the impact of preheating on the FT-A for a particular NG injection rate. Taking this slope and plotting it against the NG injection rates, as shown in Figure 10, provides an indication of the impact of preheating as a function of the injection rate. The impact of the preheating increases gradually to a peak impact of 0.177 K increase in FT-A per 1 K of NG preheat at an injection rate 105 kg/THM before declining as the injection rate increases past 105 kg/THM (Figure 11).

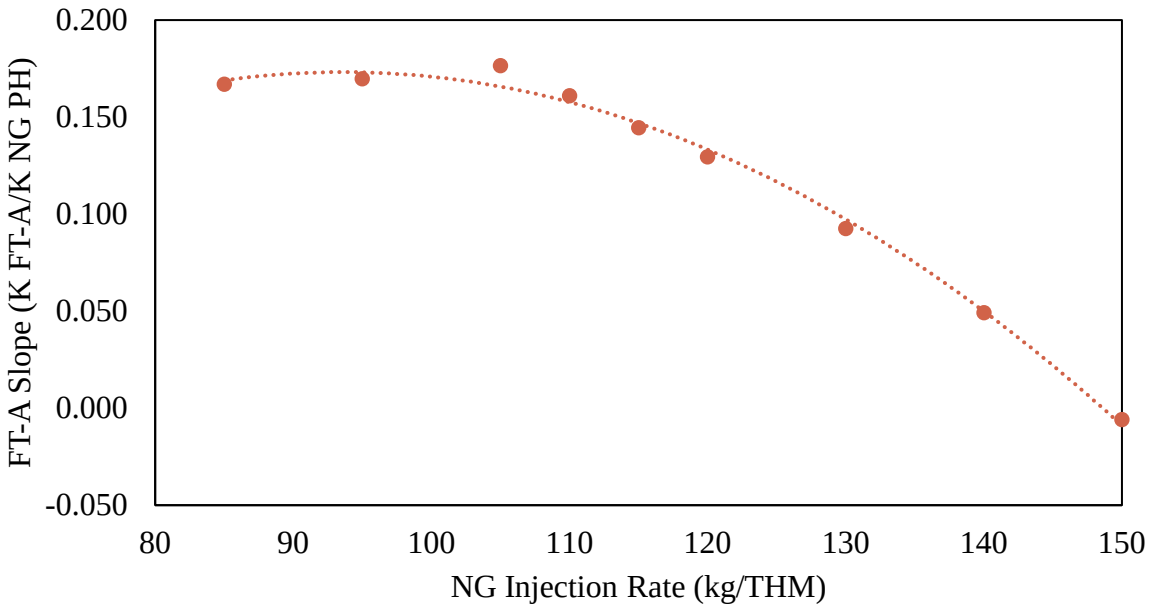

Figure 11: NG preheating efficiency vs. NG injection rate

This phenomenon of decreasing residence time in the tuyere and raceway also provides a potential explanation for the decreased impact of NG preheating as the injection rate increases beyond 105 kg/THM. It is noteworthy that in the CFD models the gases are treated as incompressible ideal-gases, with a variable density model in place. Thus doubling the gas temperature (i.e. a 300K preheat with a baseline temperature of 300K) will halve the density of the gas, leading to a corresponding increase in velocity. This suggests that there are competing mechanisms at work, where preheating is increasing the amount of sensible heat entering the furnace and improving the mixing and combustion of the NG, and the increased gas velocity is reducing the residence time of the NG in the raceway envelope and potentially leading to additional cracking.

Figure 12 depicts the cracking rate was calculated for the 0 K and 300 K preheat cases for each injection rate and is normalized relative to the rate of NG cracking in the baseline case with 0K PH to investigate CH_4 decomposition in the raceway region. This indicates an overall increase in the CH_4 cracking rate relative to the baseline injection rate with no preheat, however it is important to note that this is total amount of NG that is cracking, not a percentage of injected NG. Figure 13 compares these normalized cracking rates, and plots the increase in CH_4 decomposition with preheating, as a function of the injection rate.

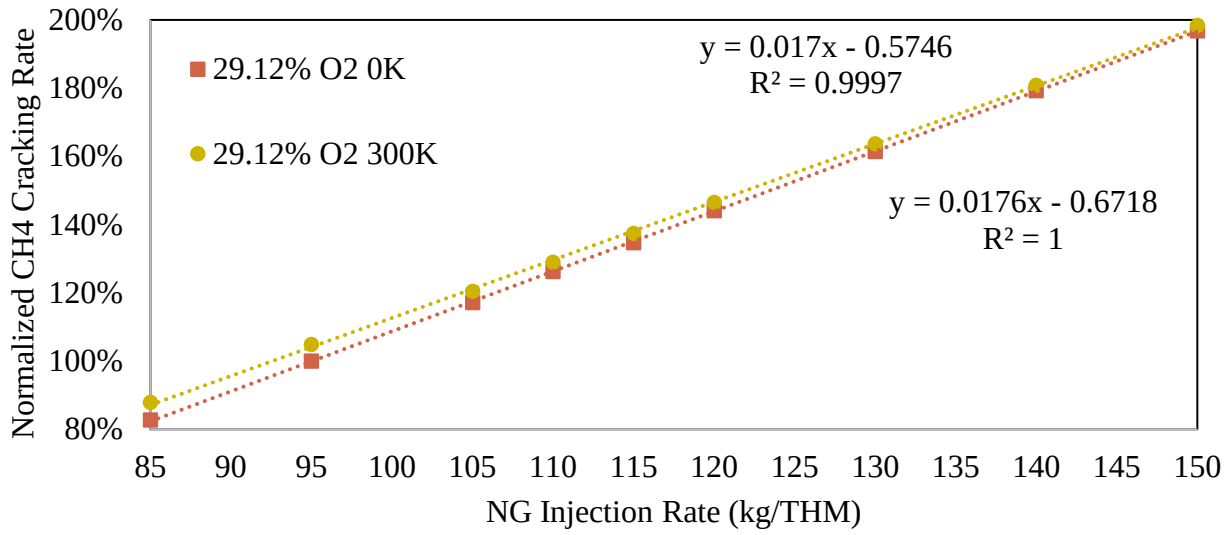

Figure 12: Normalized CH_4 cracking rate in the raceway vs NG injection rate

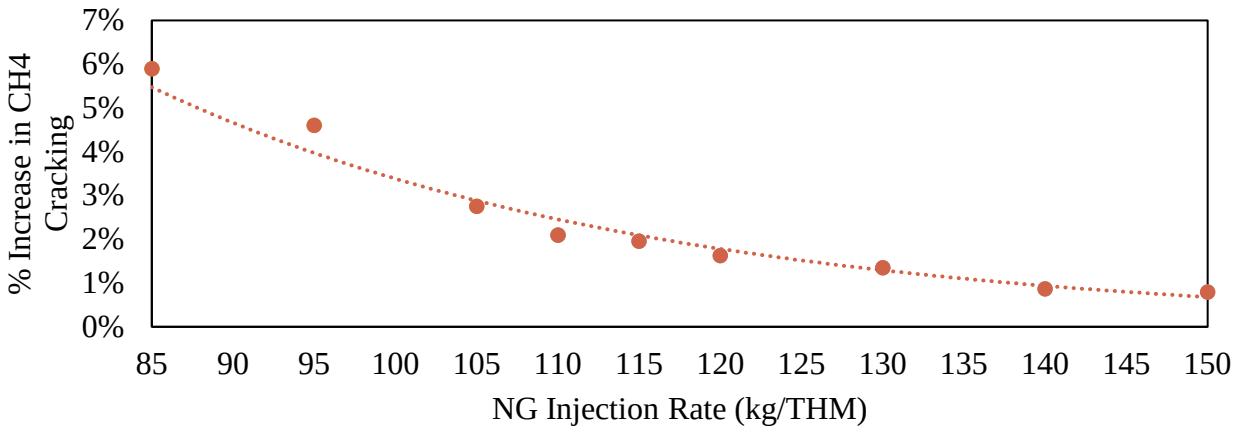

Figure 13: Increase in CH_4 decomposition inside the raceway vs. NG rate between 0K PH and 300K PH cases at each injection rate

Shaft region modeling predicts a net positive impact on the predicted coke rate from NG preheating. The combination of increased sensible heat and improved NG combustion when preheating the NG reduced the furnace coke rate by approximately 2.5 kg/THM of coke per 100K of NG preheat. Figure 14 shows the relationship between the coke rate and the NG injection rate at various levels of preheating. The preheating appears to provide a net offset to the coke rate, with a slight reduction in the replacement ratio of the NG as the level of preheating increases.

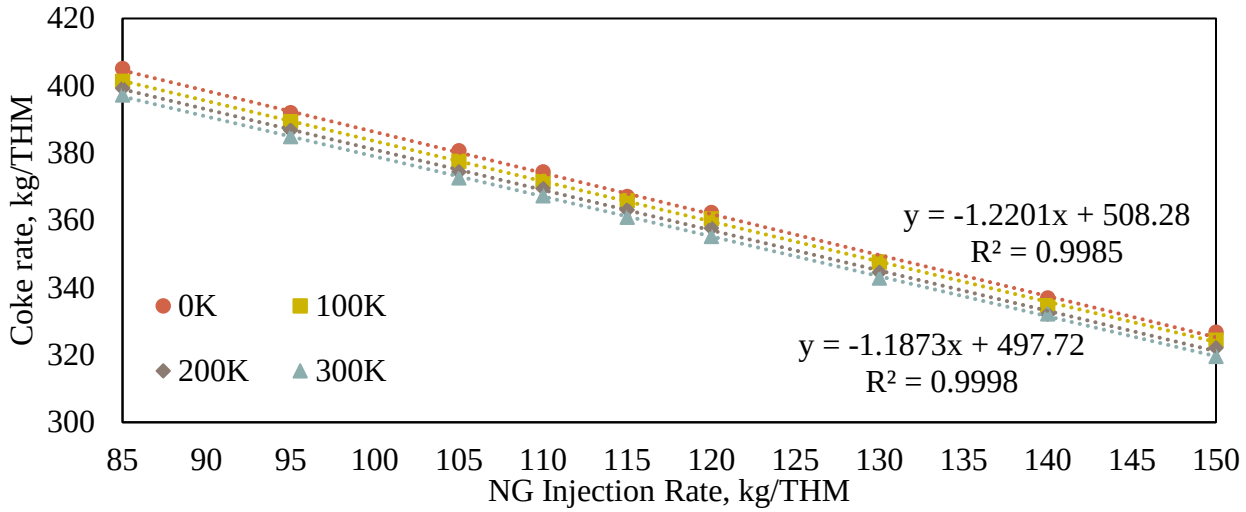

Figure 14: Coke rate vs NG injection rate at various preheat levels

The shaft model simulations also indicate increasing top gas temperature (TGT) as the amount of injected NG increases, in line with expectations from industrial operating experience (see Figure 15). The model also predicts a slight decline in average top gas temperatures as the level of NG preheating increases. As the scenarios have compared favorably to increasing hot blast temperature when looking at conditions within the raceway, this is not necessarily a surprising prediction (and it aligns well with industry rules of thumb [2]), though it remains somewhat counterintuitive.

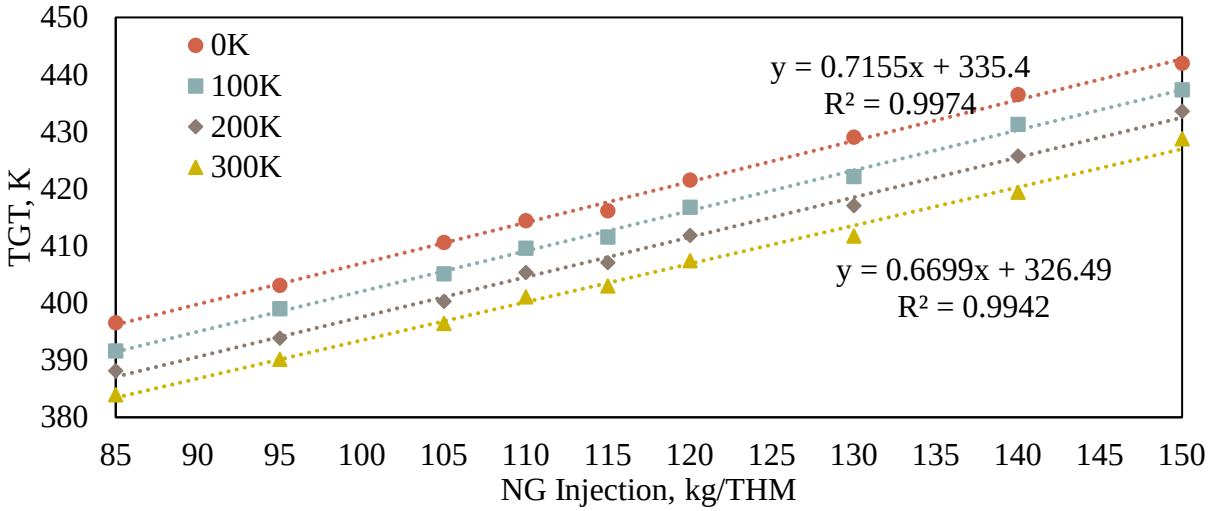

Figure 15: Top gas temperature vs NG rate at various preheat levels

5. RELATIONSHIP BETWEEN FT-A/RAFT & TOP GAS TEMPERATURE

In the course of this research an inverse trend between the RAFT/FT-A and the average top gas temperature was found in several industrial rules of thumb. This holds true for adjustments to injectants, hot blast temperature, hot blast moisture, and oxygen enrichment, suggesting that this behavior is a function of the chemical kinetics in the furnace as opposed to simply shifting chemistry. Figure 16 provides an overview of documented industrial rules of thumb for the relative impact on RAFT and TGT for a generic BF with varying injectants, hot blast temperatures, and blast moisture.

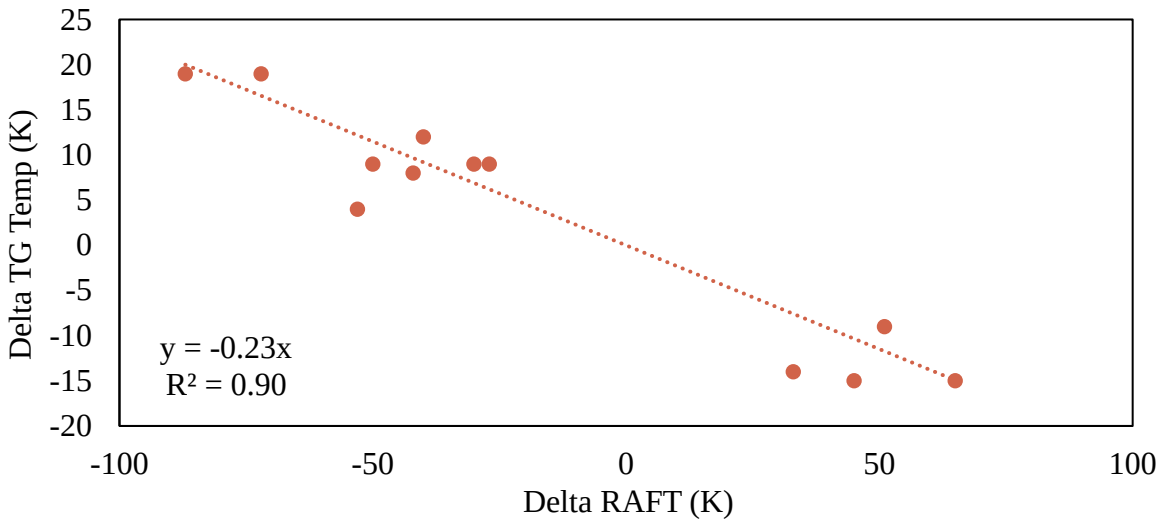

Figure 16: Industrial rule of thumb RAFT vs TGT trend [2]

Constructing a similar figure using the CFD generated data, Figure 17, it is apparent that the same trend is present. For these cases the change in FT-A and TGT from the baseline were calculated and plotted. Comparing the slopes of the resulting slopes of the best fit trend lines indicate the decrease in TGT per increase of FT-A, -0.23 K FT-A/K TGT for the industrial RoT and -0.219 K FT-A/K TGT for the CFD results, a difference of 4.7%. This suggests that there is a fundamental tradeoff between FT-A and TGT. This also serves as primitive validation, confirming that the models are predicting results in line with the trends expected from industrial experience. Some further investigation of reduction reaction kinetics for the blast furnace shaft region appears

to indicate that the higher temperatures can promote H_2 reduction as the dominant reaction for wustite (an endothermic reaction) as opposed to CO reduction (an exothermic reaction). This increased H_2 reduction could lead to the decreased top gas temperatures observed in all scenarios where FT-A rises, but further investigation is required.

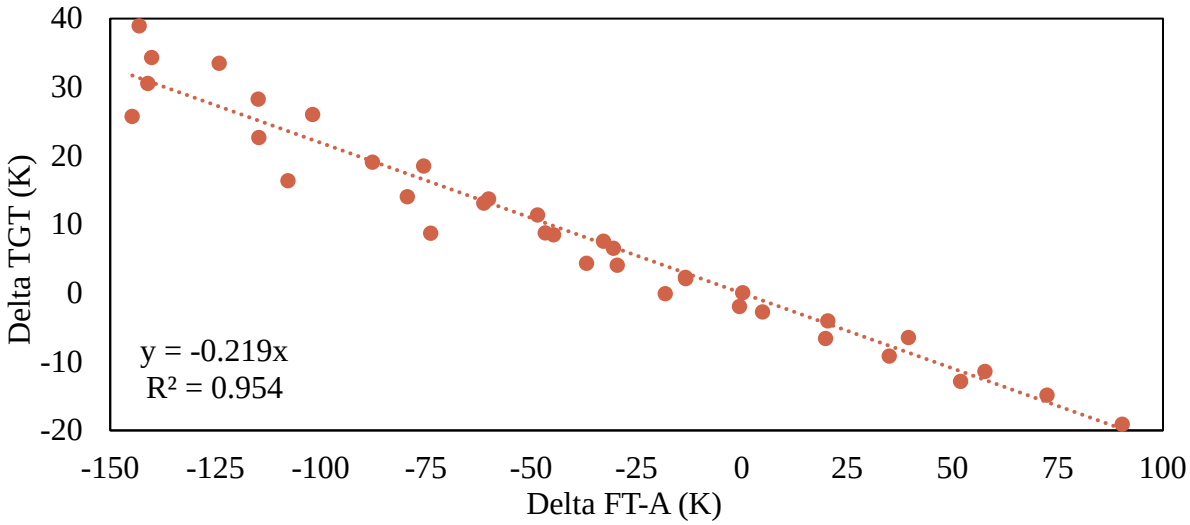

Figure 17: CFD predicted FT-A vs TGT trend

6. SYNGAS INJECTION RESULTS

Given the limitations of natural gas preheating syngas injection was investigated as a potential method for reducing carbon emissions from the BF. In the tuyere region when considering syngas injection at identical mass flow rates the baseline natural gas injection case (0.28 kg/s/tuyere), the high temperatures of the syngas cause significant shifts in the location of the syngas plume (Figure 18). At higher injection temperatures this can cause impingement on the side wall of the tuyere, and potentially cause increased thermal wear on the tuyere. Because of this it is desirable to reduce the injection velocity by reducing the temperature of the syngas to decrease the velocity. The 583K COG #1 composition case significantly reduces the impingement on the sidewall when compared to the high temperature injection.

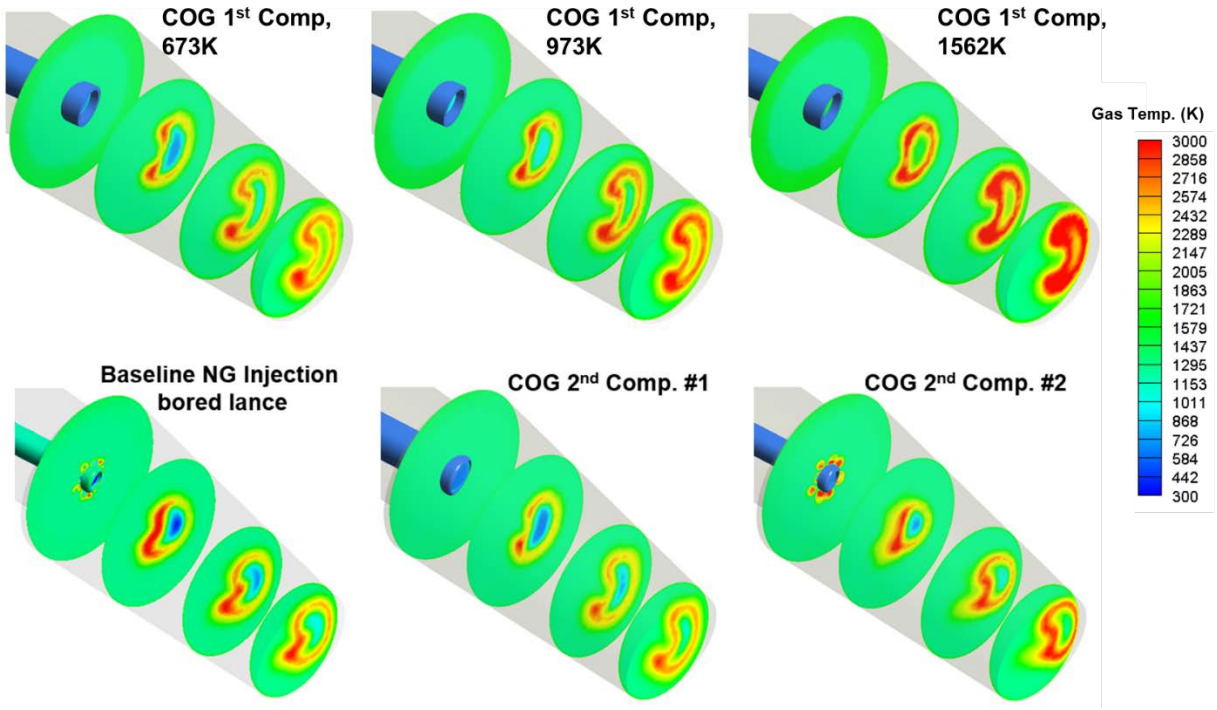

Figure 18: Comparison of gas temperature distributions in the tuyere region for different syngas compositions and injection temperatures

Moving to the raceway region syngas injection produced higher FT-A values (Figure 19). Preheating efficiency for the syngas compositions were slightly lower than the natural gas cases (0.17 FT-A K/PH K) depending on the composition. The NG feedstock case was the lowest at 0.13 FT-A K/PH K, while the COG feedstock cases were much closer to the baseline at 0.16 FT-A K/PH K. This suggests that the temperature of the syngas has a less pronounced impact on the FT-A, however because decomposition and soot deposition at high temperatures is not a concern with syngas injection it is possible to push a higher injectant temperature thus realizing a greater impact on the furnace.

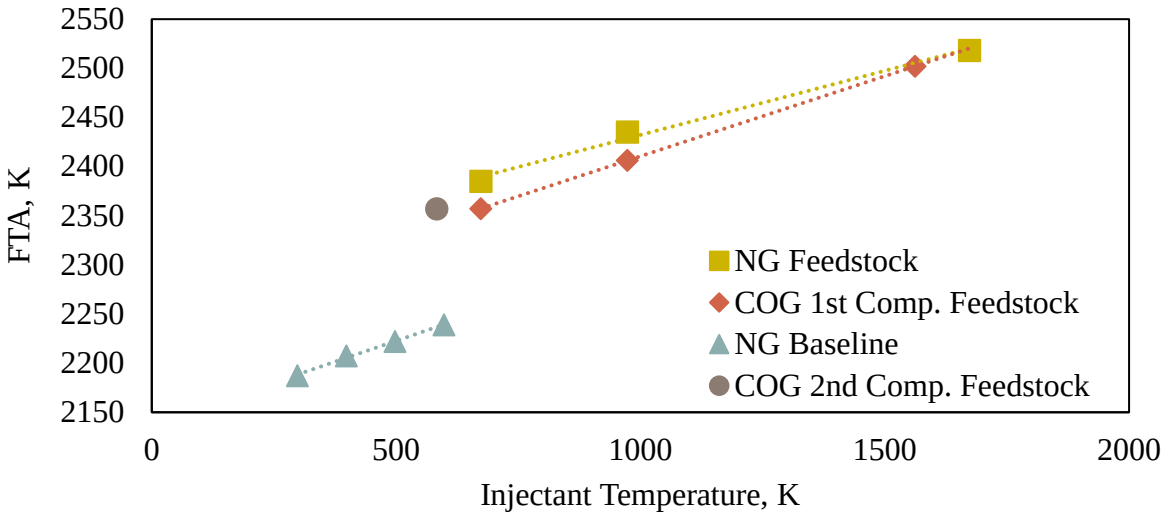

Figure 19. FT-A vs injection temperature for various syngas compositions

Gas temperatures in the raceway are uniformly higher with syngas injection (Figure 20). Because syngas injection all but eliminates the decomposition reactions for all species except H_2O and CO temperatures increase. It is also notable that because of this the left-right asymmetry that is present in the natural gas baseline case is significantly reduced, resulting in a more uniform bosh gas temperature distribution. There is a larger high temperature region in the raceway above the tuyere plume in the raceway combustion cases that is likely due to the combustion of CO.

Syngas injection also causes significant shifts in the species distributions inside the raceway. Figure 21 depicts the changes to the intermediate combustion species between the natural gas baseline and the two selected syngas cases. There is a significant increase in CO_2 over the baseline case, likely due to increased combustion in the tuyere of CO in the syngas.

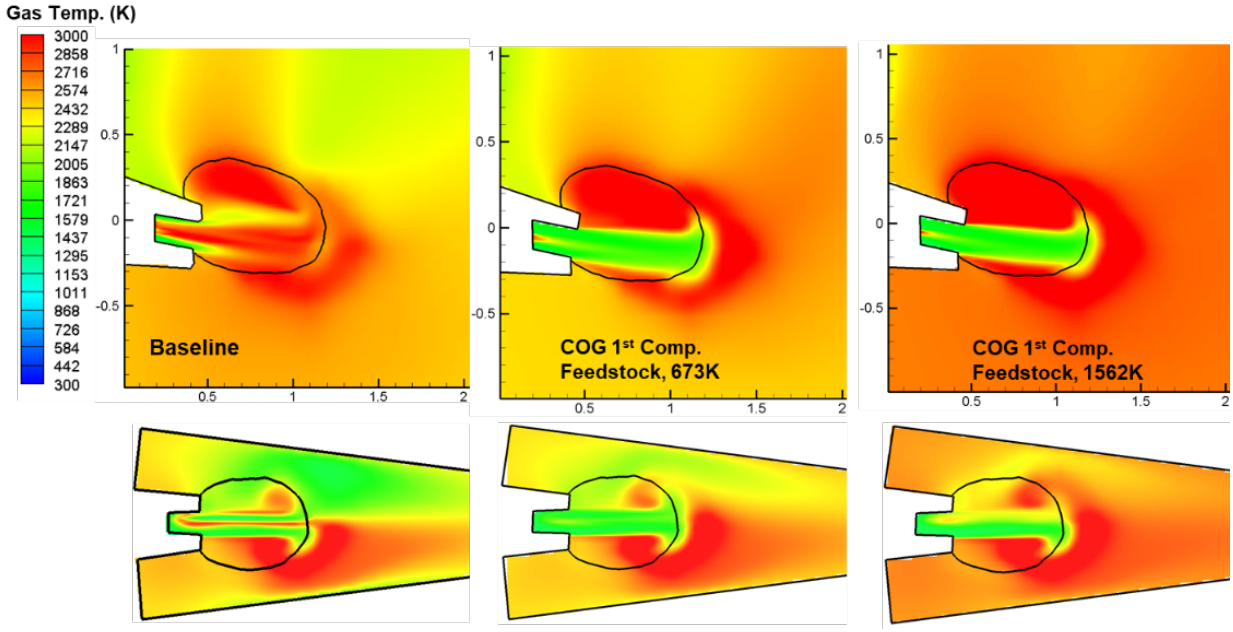

Figure 20: Gas temperature contours: Baseline NG injection (left), COG 1st comp. 673K (center), COG 1st comp. 1562K (right)

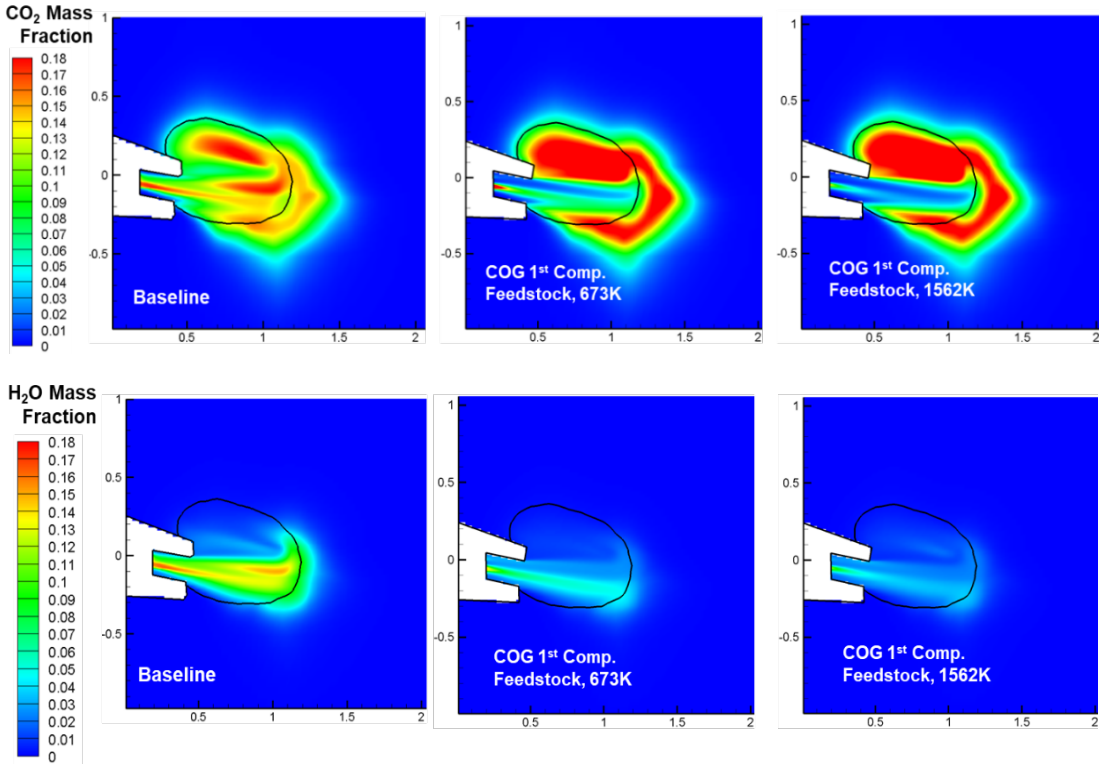

Figure 21: Gas species distributions: Baseline NG injection (left), COG 1st comp. 673K (center), COG 1st comp. 1562K (right)

Hydrogen distributions shift to the left because of the increased plume momentum, largely pushing it off the center plane. Because of this a larger concentration of water vapor is apparent in the natural gas baseline case.

Moving to the shaft region syngas injection also appears to positively impact furnace operation with significant reductions in coke rate. The lowest injection temperature NG feedstock and COG feedstock syngas cases both showed reduced coke rates from the baseline of 392 kg/THM (Figure 22 and Table 10). NG feedstock injection at 673K resulted in a predicted coke rate of 377 kg/THM an 3.8% reduction, while the COG feedstock syngas at the same temperature resulted in a reduction of 2.5% percent for a coke rate of 382 kg/THM.

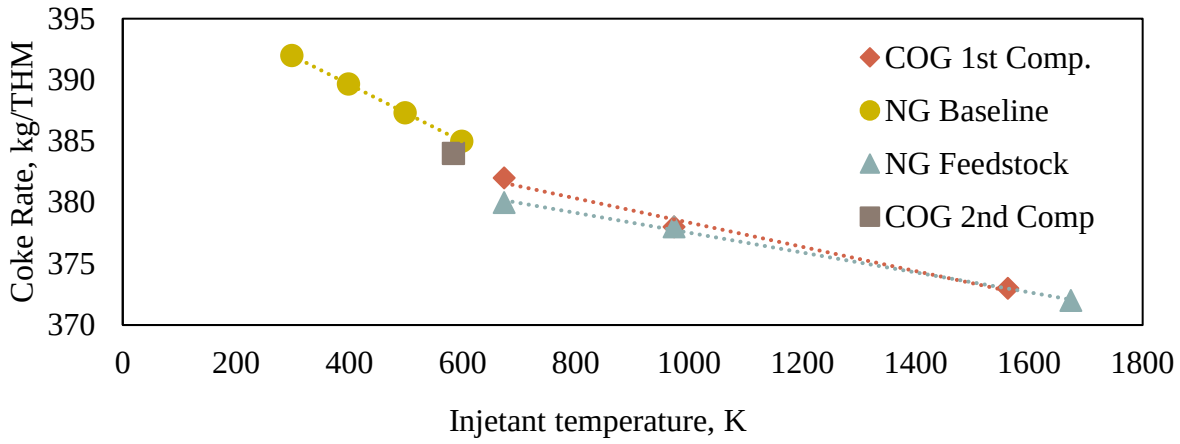

Figure 22: Coke rate vs injectant temperature with syngas injection

Table 10**:** Syngas raceway and shaft results

Case	Syngas Feedstock	Injection Temp	Syngas ṁ	FTA K	Coke Rate	TGT °C
NG Baseline	NG	392K	0.28 kg/s	2187K	392 kg/THM	130
Cooled NG Syngas – Std Lance	NG	673K	0.30 kg/s	2416K	377 kg/THM	102
Hot NG Syngas –Straight Lance	NG	1673K	0.30 kg/s	2518K	372 kg/THM	91
Cooled NG Syngas – Straight Lance	NG	673K	0.30 kg/s	2385K	380 kg/THM	104
Mid Temp. NG Syngas – Straight Lance	NG	973K	0.30 kg/s	2437K	378 kg/THM	103
Hot COG Syngas – Straight Lance	COG	1562K	0.30 kg/s	2502K	373 kg/THM	94
Cooled COG Syngas – Straight Lance	COG	673K	0.30 kg/s	2357K	382 kg/THM	108
Mid Temp. COG Syngas – Straight Lance	COG	973K	0.30 kg/s	2406K	378 kg/THM	103
COG 2nd Comp. Syngas – Straight Lance	COG	583K	0.30 kg/s	2323K	384 kg/THM	112
COG 2nd Comp. Syngas – Std Lance	COG	583K	0.30 kg/s	2357K	382 kg/THM	111

To investigate the quenching effect of increased syngas injection six case series were constructed using the three syngas compositions. In the COG #1 syngas cases and the NG feedstock syngas cases the oxygen content of the hot blast was held constant and the injection temperature varied between the "hot" temperatures obtained by injection immediately after the syngas generator, and a colder 673K injection temperature. The two cases with the COG 2nd composition syngas were both injected at the same temperature of 583K but the oxygen content was modified. In one with the oxygen content of the hot blast held constant and one with the oxygen enrichment in the hot blast reduced to maintain the same coke consumption in the raceway as the baseline natural gas case. The syngas injection rate was varied between 80 and 150 kg/THM. As with the fixed injection rate syngas cases significant wall impingement was noted at higher temperatures and injection rates, suggesting that other design modifications may need to be implemented to prevent damage to the tuyeres.

Moving to the raceway syngas injection presents a significant potential to boost FT-A. COG 1st composition syngas injection appears to have a reduced impact on FT-A over both ambient and preheated natural gas, suggesting the potential to push higher injection rates with reduced quenching effects on the furnace. The impact on FT-A is increased with cooler temperature syngas injection due to the reduced sensible heat entering the furnace. Both syngas temperatures result in FT-A values significantly above NG injection at comparable rates (Figure 23).

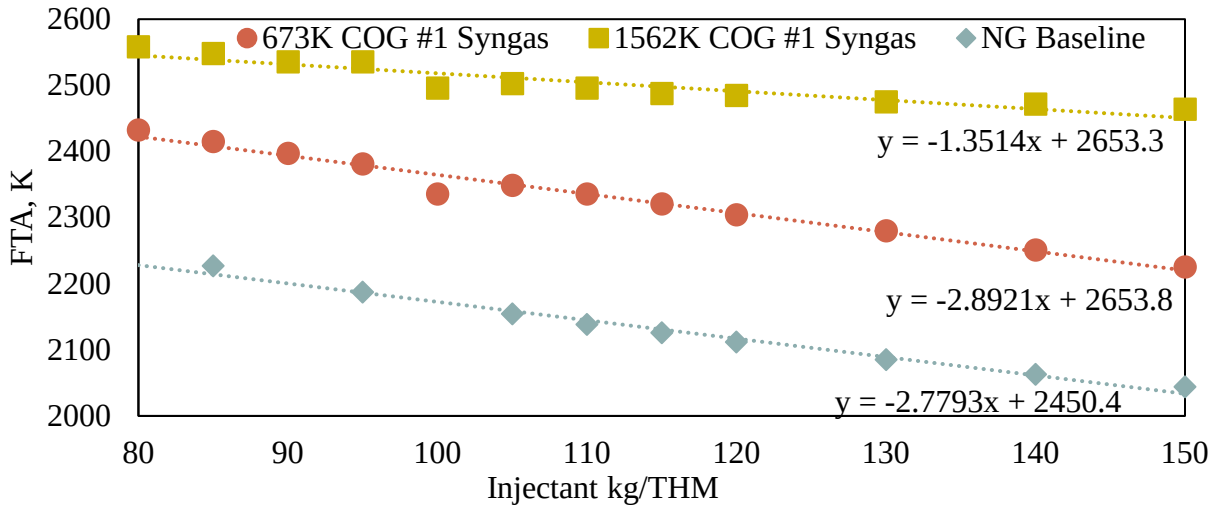

Figure 23: Syngas COG composition #1: FT-A vs injection rate

With the NG feedstock syngas, the higher temperature injection cases the predicted quenching effect is -0.69 K FT-A per 1 kg/THM increase in syngas flow rate vs the NG baseline of -2.78 and the predicted COG feedstock syngas composition #1 of -1.35 at the higher injection temperature (Figure 24). It is important to note that the NG feedstock syngas is entering the furnace 111K hotter than the COG feedstock syngas composition #1. The reduction in quenching effect is likely due to the increased oxygen flow into the furnace resulting in increased coke consumption in the raceway resulting in higher gas temperatures and a likely increase in the coke rate of the furnace.

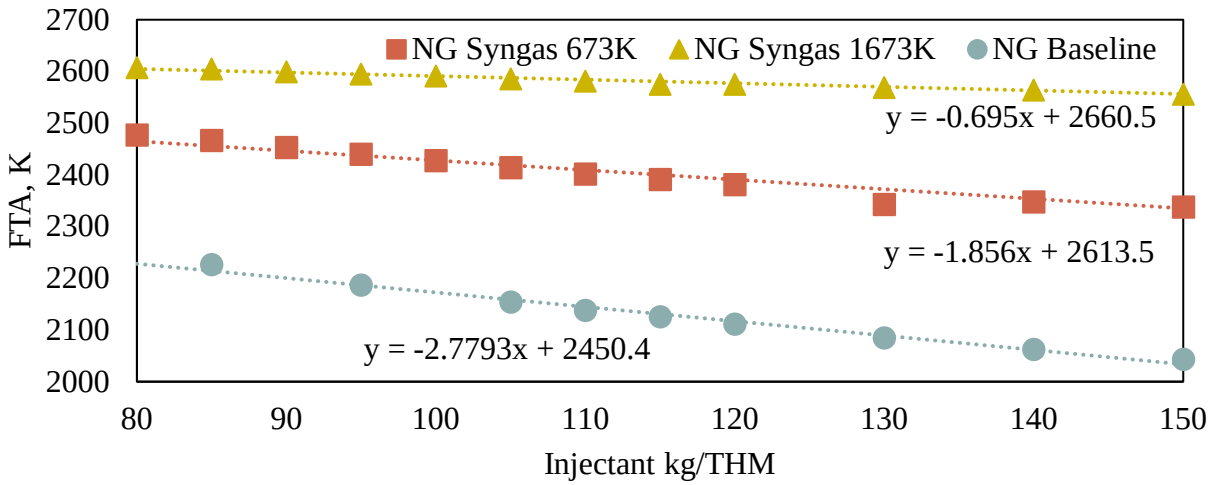

Figure 24: NG syngas: FT-A vs injection rate

The third syngas composition is the COG feedstock composition #2, which was calculated as a COG sygnas that was quenched after combustion to lower the temperature. Here the injection temperature is reduced to 583K from the 1562K and 1673K of the two other syngas compositions. This results in slightly lower temperatures while maintaining lower quenching effect than traditional NG injection at -2.98 K FT-A per 1 kg/THM of syngas injection (Figure 25). Because of the easier implementation of cooler syngas injection without significant retrofitting operations at an existing furnace this syngas composition was selected for several additional case series to try and pin down the particulars of BF operation with syngas. The first significant adjustment was to reduce the oxygen content of the hot blast by the amount of oxygen consumed in the hypothetical syngas reactor so a constant amount of oxygen was entering the furnace. This removed amount will increase as the syngas mass flow rate increases.

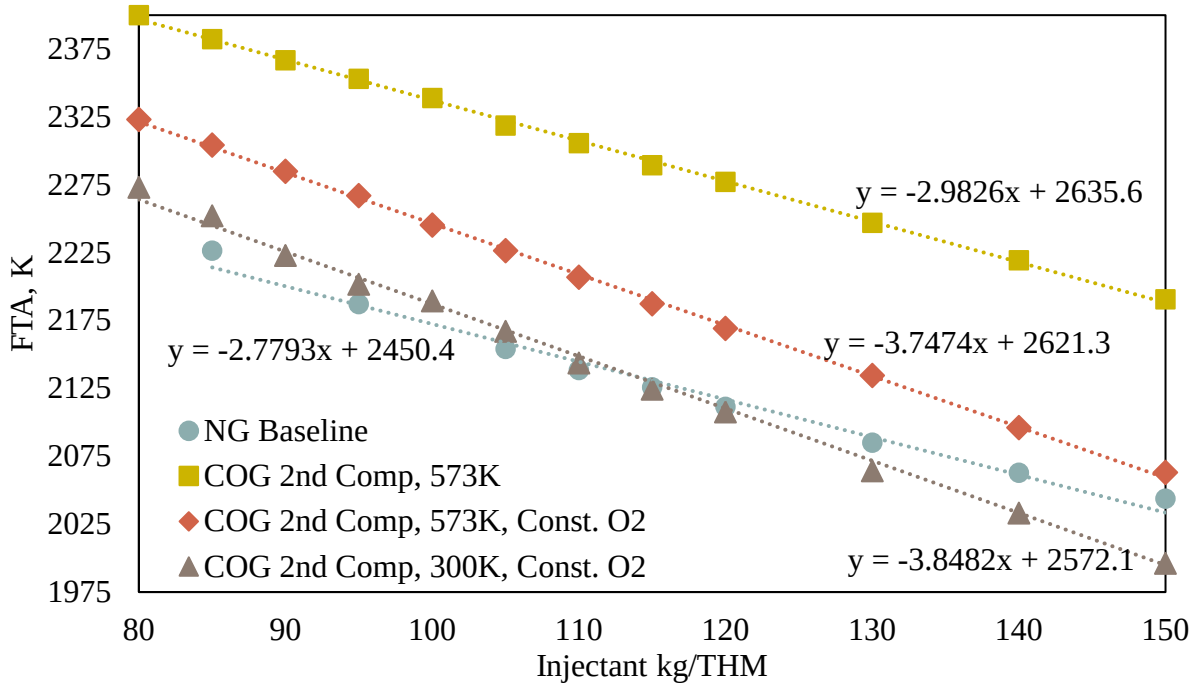

Figure 25: Syngas COG composition #2: FT-A vs injection rate

In these "constant O_2" cases the hot blast oxygen enrichment was reduced by the amount of oxygen consumed in the hypothetical syngas reactor, effectively diverting oxygen from the hot blast to the syngas reactor, and keeping a constant amount of oxygen atoms entering the furnace, albeit in different species than O_2. The initial constant oxygen case at 583K showed a decline of approximately 90K over the initial "fixed oxygen" case series for COG composition #2 syngas at the same temperature, see Figure 25. The constant oxygen case series also showed a moderately higher quenching effect on FT-A compared to the fixed oxygen case series (-3.75 vs. -2.98 respectively). This is likely due to the reduction in sensible heat entering the BF as the amount of oxygen entering the blast furnace declines.

This oxygen adjustment is designed to control the coke consumption in the raceway, this will reduce the FT-A, which would be offset by the increase in FT-A from hot syngas injection, potentially allowing a higher injection rate over the NG baseline while maintaining FT-A, and reducing coke rate. Given the relatively similar FT-A values between the 583K COG syngas #2, constant oxygen case series and the 300K PH NG case series a third case series was run using the constant oxygen adjustments and lowering the injection temperature of the syngas to 300K (~25 °C) to directly compare the impact of the syngas chemistry versus the baseline natural gas injection.

This results in higher FT-A temperatures with natural gas injection below a 110 kg/THM injection rate. As the injection rate is increased, the reduced oxygen syngas begins to produce higher FT-A temperatures. This is likely due to the increase in cracking as the NG injection rate increases. By virtue of being pre-combusted the syngas is free from this limitation on higher injection rates.

7. HYDROGEN INJECTION

The positive impacts on syngas injection lead to inquire into the potential for hydrogen injection in the BF. Hydrogen injection presents several fundamental differences. Firstly is that pre-reformed reducing gas is being directly injected into the furnace, removing any heat quenching decomposition reactions, and renders the "burnout" of the hydrogen largely a moot point. Secondly hydrogen's much lower density will result in higher injection velocities.

Existing literature indicates that hydrogen injection can pose several significant issues to the operation of the furnace [7-9]. Because pre-reduced reducing gas is being injected there is little benefit to combustion, as any products will almost immediately decompose once they enter the coke bed, returning to H_2 and reacting with coke to create CO. This coupled with the loss of a carbon stream from any prior natural gas injection leads to a furnace that is generally colder than a comparable NG furnace. Methods to counter this are needed if hydrogen injection is going to become a viable technology. Several were investigated in this research, most prominently preheating and co-injection.

Initial investigation consisted of straight replacement of NG injection with hydrogen. Using the same methodology as previous investigations, a range of injection rates from 5kg/THM to 35 kg/THM were tested. In the tuyere region one consistent finding was present; the low density of hydrogen allowed for extremely high injection velocities without high temperature impingement on the side wall of the tuyere (Figure 26). This is likely a result of the low density of hydrogen relative to the hot blast. The total momentum carried by the H_2 plume is so small compared to the momentum of the hot blast that the hydrogen plume remains centered in the tuyere. This was present across all hydrogen cases in the matrix. This finding suggests that preheating may be more viable with hydrogen, as compared to NG.

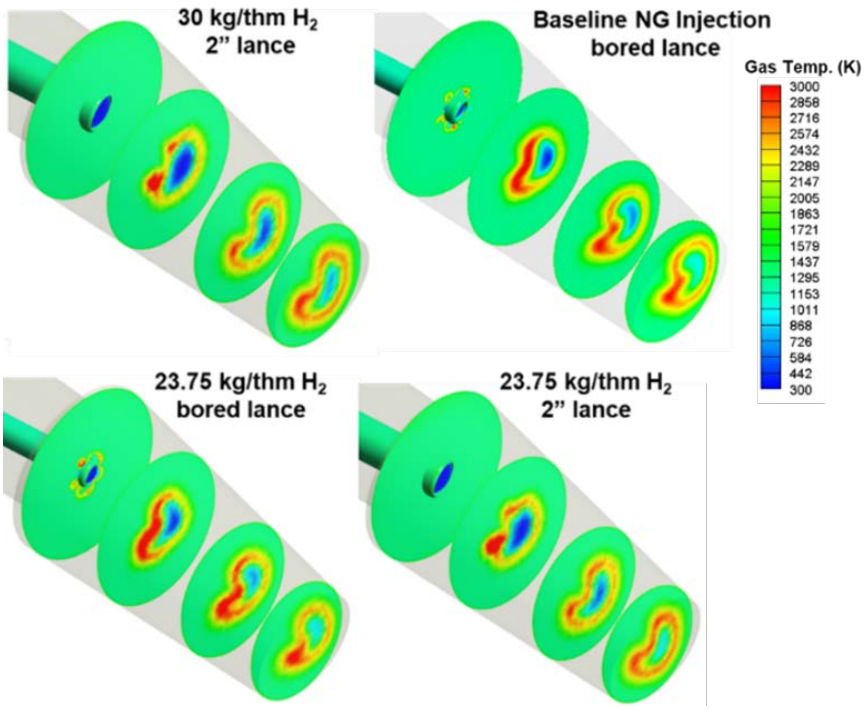

Figure 26: Comparison of tuyere gas temperatures 30kg/THM H_2 straight lance (upper left), baseline NG injection bored lance (upper left), 23.75 kg/THM H_2 bored lance (lower left), 23.75 kg/THM H_2 straight lance (lower right)

Looking towards the raceway hydrogen injection tends to lead to higher temperatures, this is likely an artifact of the assumptions in the modeling process. The hydrogen content of the bosh gas is governed by the injection conditions at the tuyere, and the total amount of hydrogen entering the furnace, either through auxiliary fuels, or humidity in the hot blast. The CO content is governed by the amount of oxygen in the hot blast. In this initial modeling work the oxygen content of the hot blast was not adjusted. This was a conscious choice to maintain similar bosh gas chemistry, and to reduce the number of variables being investigated. Because of this decision the carbon that had been previously supplied by the NG injection must now be supplied by the coke bed surrounding the raceway. For the baseline NG injection rate of 95 kg/THM a total of 71.25 kg/THM of carbon is supplied to the furnace. This increased coke consumption in the raceway will directly impact the coke rate of the BF, and leads to one of the fundamental issues with hydrogen injection. Fundamental reductions in carbon emissions require that hydrogen replace CO as a reducing gas in fairly large quantities. Given the energy intensive process of manufacturing coke,

in some scenarios it may result in fewer carbon emissions to use traditional NG injection, when compared to hydrogen injection without significant hot blast oxygen adjustments.

In the raceway region the impact of the increased coke consumption and higher temperatures is apparent. Hydrogen injection produces FT-A values that are approximately 200K higher than comparable molar injection rates of NG. This indicates the possibility of adjusting the O_2 content of the hot blast to reduce temperatures and coke consumption in the raceway. Figure 27 outlines these trends, and also provides a comparisons of the mass basis injection rates that would be required to match a particular molar bosh gas flow rate for a particular NG injection rate. There is relatively little change to overall flow conditions in the RW as the hydrogen injection rate increased.

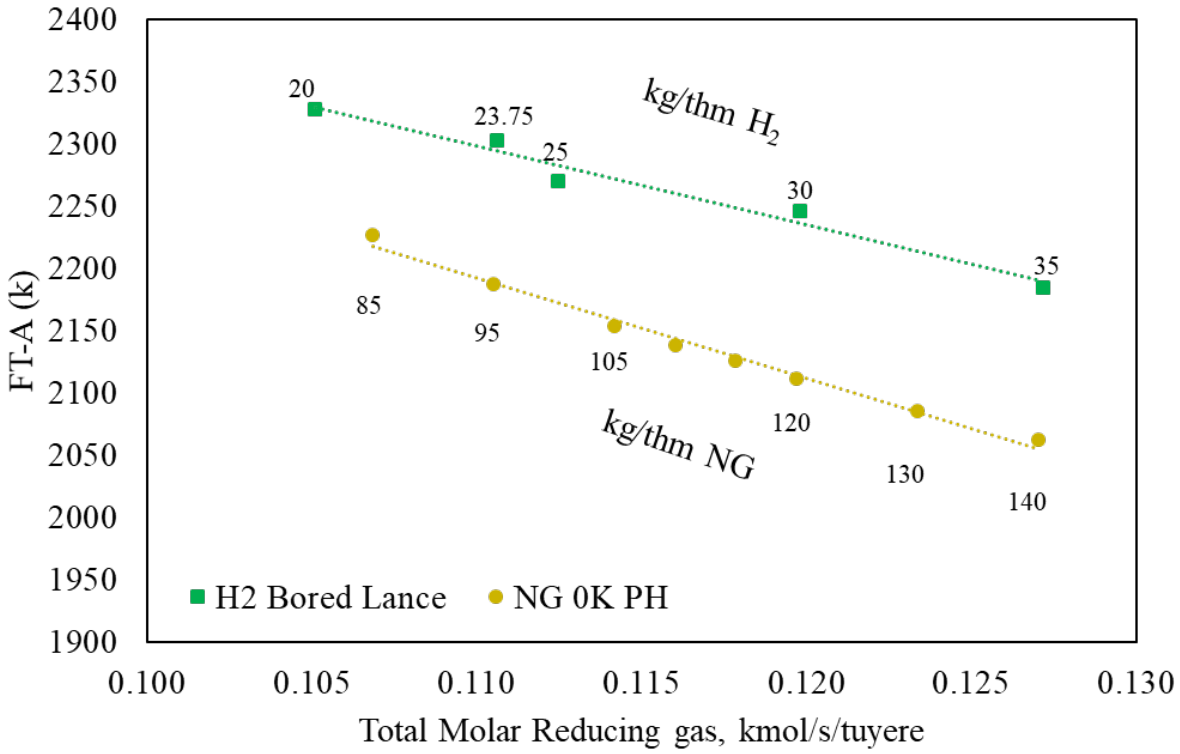

Figure 27: FT-A vs reducing gas molar flow rate for both hydrogen and natural gas injection

In the shaft region the impacts of increased coke consumption become apparent, with significantly increased coke rates over the baseline of 392 kg/THM (Figure 28), however the total carbon rate of the furnace is a more useful metric for comparison. Accounting for the 95 kg/THM of natural gas injected in the baseline case, an additional 71.25 kg/THM of carbon is provided to

the furnace, for a total carbon rate of 463.25 kg/THM. For the hydrogen cases the carbon rate is the coke rate. This indicates that at hydrogen injection levels above 30 kg/THM there will be a net reduction in carbon emissions for this furnace at these operating conditions. Results for top gas temperature also indicate that above 30kg/THM there is sufficient top heat to prevent condensation. Hydrogen injection appears to results in a less uniform temperature distribution of bosh gas (Figure 30). It also causes the cohesive zone to sit approximately 4 meters lower in the furnace.

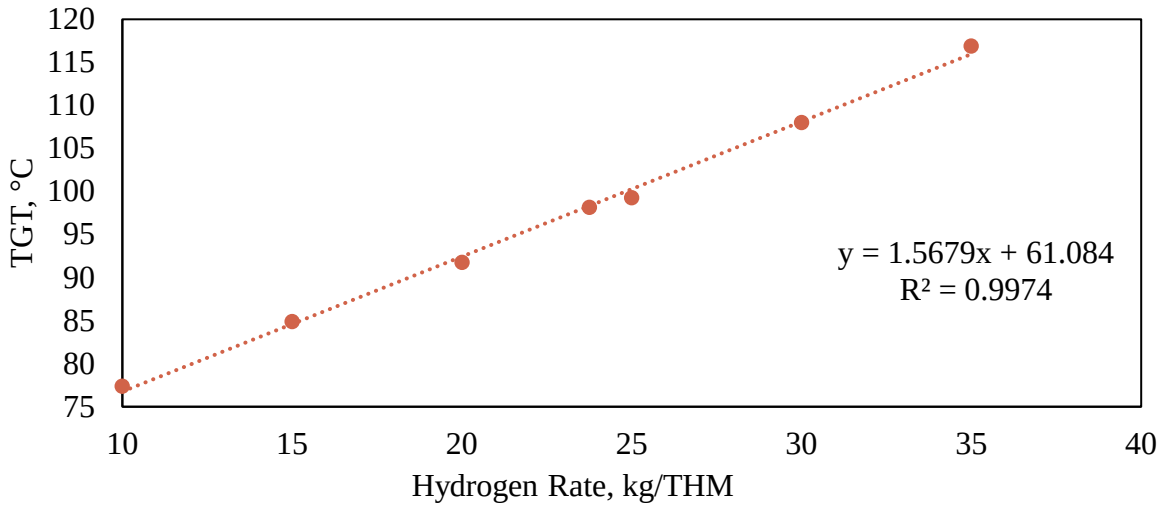

Figure 28, TGT vs H_2 injection rate

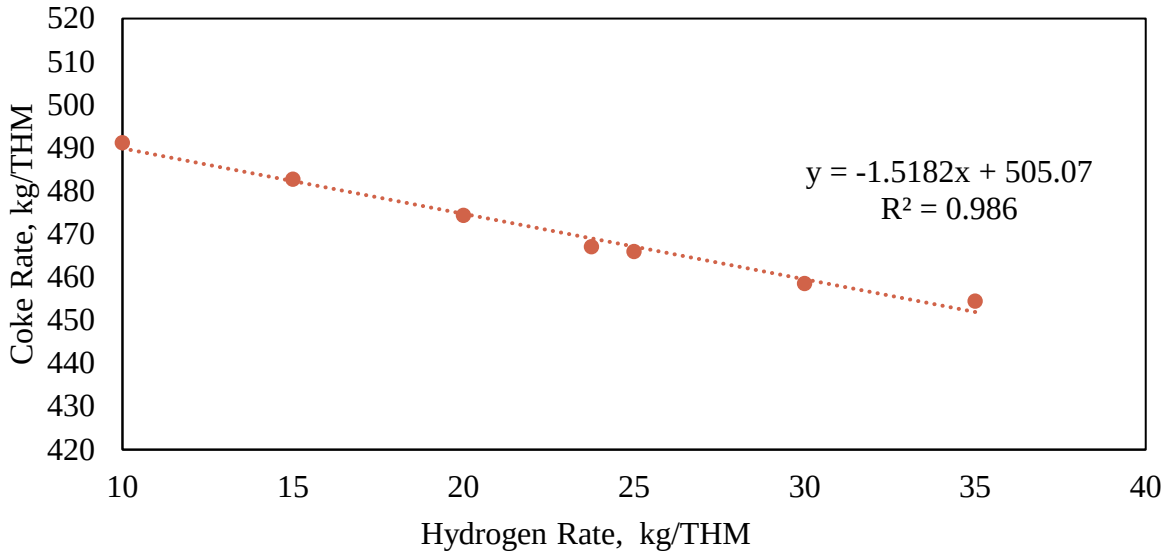

Figure 29: Coke rate vs H_2 injection rate

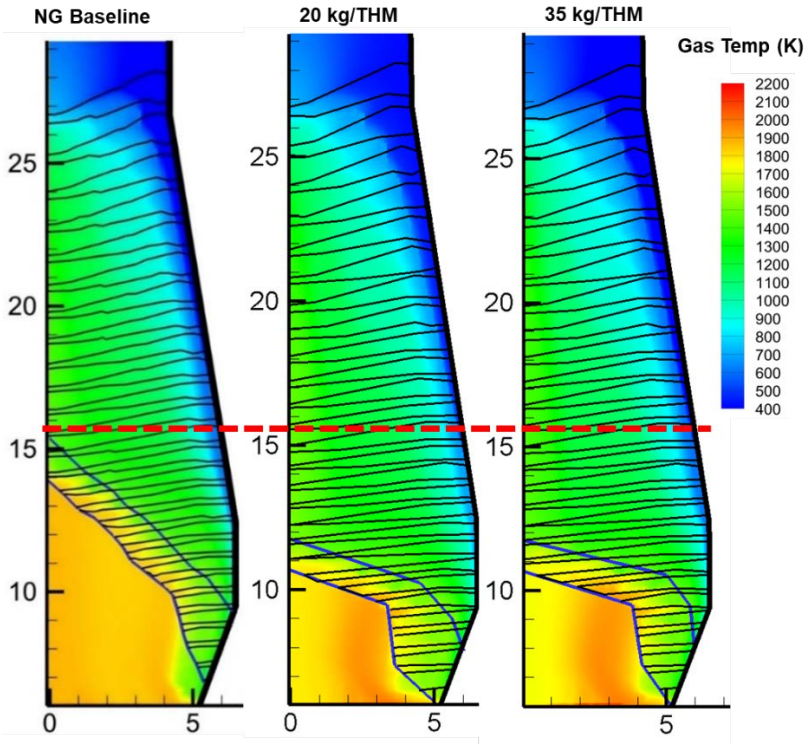

Figure 30: Cohesive zone migration and shaft region gas temperature contours: natural gas baseline (left), 20 kg/THM H_2 (center), 35 kg/THM (right)

Building on the previously discussed natural gas preheating work, hydrogen preheating was explored as a method of increasing the sensible heat entering the furnace. Hydrogen preheating was only modeled through the raceway, however the results still illustrate the increased sensible heat in the furnace. One particularly noteworthy result is the relatively minor impact on plume location, Figure 31, even at very high preheats the hydrogen plume remains centrally located in the tuyere with no impingement on the side walls. This overcomes the difficulties with high temperature and injection rate natural gas and syngas injection.

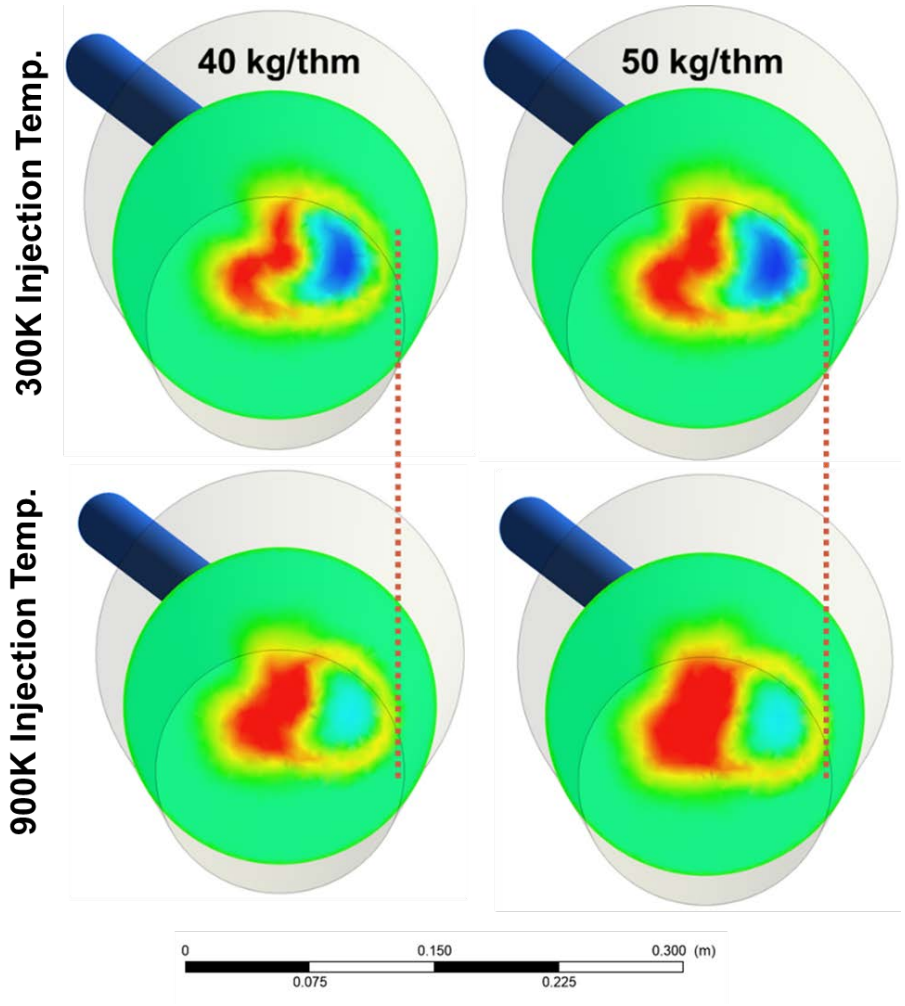

Figure 31: Fuel plume migration with hydrogen preheating

In the RW temperatures (Figure 32) were consistently higher with preheating, in some cases reaching FT-A values comparable to NG injection. Here the preheating efficiency is significantly higher than for preheating with comparable NG injection rates. The preheating efficiency of the baseline 95 kg/THM natural gas injection cases was found to be 0.17 K FT-A per K preheat, the three hydrogen preheating cases averaged a preheating efficiency of 0.5 K FT-A per K preheat, providing significantly improved realization of the goal of increased sensible heat in the furnace. This suggests that even higher temperature injection may be possible, with corresponding benefits from the increased sensible heat entering the BF.

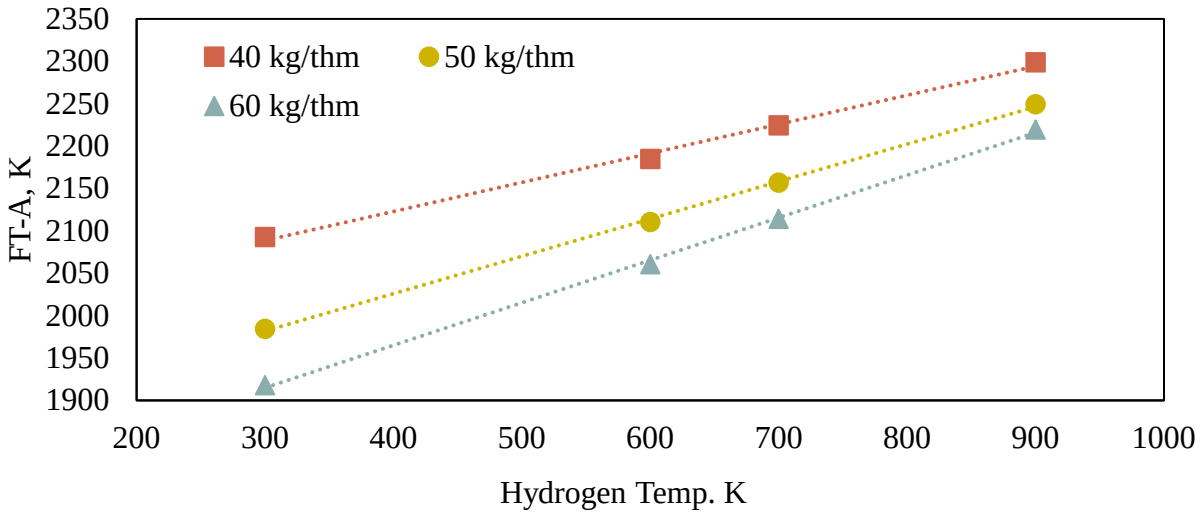

Figure 32: FT-A vs injectant temperature, hydrogen preheating

8. DISCUSSION AND CONCLUSIONS

Potential Economic Benefits

Assuming a cost of $118.30/kNm^3 ($3.35 per thousand SCF) for natural gas, an coke price of $275/metric ton ($250/short ton, and a production of 6580 THM/day (7253 short tons of hm/day), and taking cases with similar FT-A and TGT to the baseline case the range of potential savings is presented in Table 11. Increasing the NG injection rate to 110 kg/THM and supplying a 300K preheat will match the baseline case for FT-A and TGT, while providing a reduction in coke rate of 25 kg/THM, including the additional cost of the increased NG, this would result in an annual savings of approximately $9.9 million, vs the $4.7 million savings that could be realized through preheating alone without the increased NG injection. Given the strongly coupled relationship between the FT-A and TGT this is likely the major application of NG preheating.

Table 11: NG preheating economic impacts

NG Rate, kg/THM	NG PH, K	FT-A, K	TGT, K	Coke Rate, kg/THM	Annual Savings, USD
95	0	2187	403	392	-
95	300	2239	390	385	**$4.7M**
105	200	2192	400	375	**$7.3M**
110	300	2186	401	367	**$9.9M**

Implementation of syngas injection will require significantly more upgrades to an existing furnace, and the particulars of syngas composition and temperature will largely depend on the cost and availability of gaseous fuels at the particular plant making details of economic impact more difficult to quantify

Carbon Emissions Benefits

Among the three methods investigated in this research syngas consistently provided the best reductions in carbon emissions of the three technologies evaluated. Table 12 provides a brief outline of 8 cases that maintained reasonable FT-A values, and a TGT sufficient to prevent condensation, with the exception of the one hydrogen case. None of the ambient temperature hydrogen cases achieved a top gas temperature of above 97 °C, indicating that additional work is needed to explore the operating window for hydrogen injection.

Table 12: Summary of emission reduction

Fuel	Case	Coke Rate, kg/THM	FT-A °C	TGT °C	GHG Emissions, tons CO_2/ton steel	Emission Reduction
Natural Gas Preheating	95 kg/THM NG 0K PH	392	1914	130	1699	-
	95 kg/THM NG 300K PH	385	1966	117	1673	1.5%
	105 kg/THM NG 200K PH	375	1919	127	1664	2.1%
	110 kg/THM NG 300K PH	367	1913	128	1648	3.0%
Syngas	COG 1st comp 673K	382	2084	108	1492	12.2%
	NG feed 673K	380	2112	104	1512	11.0%
	COG 2nd 583K	382	2084	111	1517	10.7%
Hydrogen	30 kg/THM H_2 0K PH	444	2177	91	1627	4.2%

Conclusions

All of the methods outlined in this study provide a potential to reduce carbon emissions from the blast furnace, while potentially reducing operating expenses. Natural gas preheating shows promise as a method to obtain moderate improvements in efficiency, with relatively minor modification required. It is however, limited by the thermal decomposition of the natural gas at temperatures above 900K (~630°C), due to the potential for soot collection in the supply apparatus.

Syngas injection showed significant promise as an auxiliary fuel, because precombustion thermal decomposition and soot accumulation are not relevant. When one considers the high temperature of the syngas, and the associated equipment needed to implement the syngas injection it appears less desirable.

Lastly, hydrogen injection provides a method of supplying raw cold reducing gas to the furnace. Hydrogen by nature of its chemistry cannot deposit soot into supply lines, making it hypothetically possible to preheat to very high temperatures to boost sensible heat in the furnace. The primary disadvantage of hydrogen injection is that because you are injecting raw reducing gas there is no thermal benefit to its combustion in the tuyere and raceway. It must be heated by the surrounding gases resulting from coke combustion to reach the temperatures needed in the furnace.

Future Work

Future work in this research could include the impacts in the shaft region of hydrogen preheating. It is possible using hydrogen preheating in combination with several other small changes to the operating conditions of the furnace could yield a stable set of conditions. The impacts of even higher temperature hydrogen injection could also be an avenue for exploration.

Hydrogen enriched syngas may also be a viable route to boost sensible heat entering the furnace and to increase the hydrogen to carbon ratio in the bosh gas. This idea could also be extended to hydrogen enriched natural gas injection. Modifications to the geometry of the injection lances could yield a geometry better suited for high temperature and high rate injection of auxiliary fuels. This could potentially expand the range of temperatures and injection rates that could be achieved, while mitigating the concerns of high temperature impingement on the tuyere side walls.

REFERENCES

1. World Steel; *Steel Statistical Yearbook 2020 Concise version*
2. Geerdes, M.; Chigneau, R.; Kurunov, I.; Lingiardi, O.; Ricketts, J. *Modern Blast Furnace Ironmaking: An Introduction*, 2nd ed.; IOS Press: Amsterdam, The Netherlands, 2015; pp. 59-75.
3. Pistorius, P.C.; Gibson, J.; Jampani, M.; Natural Gas Utilization in Blast Furnace Ironmaking: Tuyère Injection, Shaft Injection and Prereduction. *Applications of Process Engineering Principles in Materials Processing, Energy and Environmental Technologies* 2017, pp. 283-292.
4. Feshchenko, S.A.; Pleshkov, V.I.; Lizunov, B.N.; Lapshin, A.A.; Soveiko, K.N.; Loginov, V.N.; Vasil'ev, L.E. Making Blast-Furnace Smelting More Efficient through the Injection of Heated Natural Gas. *Metallurgist* **2007**, *Vol. 51*, pp. 605-611.
5. Feshchenko, S.A.; Pleshkov, V.I.; Loginov, V.N.; Kurunov, I.F. Synergetic Effect of Natural Gas Pre-heating Prior to its Injection into a Blast Furnace. Proceedings of AISTech 2008, Pittsburgh, PA, U.S.A., May 5-8, 2008, 6 pgs.
6. Okosun, T.; Nielson, S.; D'Alessio, J.; Ray, S.; Street, S.; Zhou, C. On the Impacts of Pre-Heated Natural Gas Injection in Blast Furnaces. *Processes* 2020, *8*, 771. https://doi.org/10.3390/pr8070771
7. Linden, H.; Brooks, C.; Miller, L. Production of Natural Gas Substitutes by Thermal Cracking of Natural Gas. Liquids. *Ind. Eng. Chem.* 1955, 47, 12, 2475–2478 Publication Date: December 1, 1955 https://doi.org/10.1021/ie50552a032
8. Thyssenkrup *Injection of hydrogen into blast furnace: thyssenkrup Steel concludes first test phase successfully.* Press Release February 2 2021. https://www.thyssenkrupp-steel.com/en/newsroom/press-releases/thyssenkrupp-steel-schliesst-erste-versuchsphase-erfolgreich-ab.html
9. Yilmaz, C.; Wendelstorf, J.; Turek, T, Modeling and simulation of hydrogen injection into a blast furnace to reduce carbon dioxide emissions, *Journal of Cleaner Production*, Volume 154, 2017 , Pages 488-501, ISSN 0959-6526,
10. Rist, A., Meysson, N. A dual graphic representation of the blast-furnace mass and heat balances. *JOM 19*, 50–59 (1967). https://doi.org/10.1007/BF03378564
11. Zhen, M.; Zhou, Z; Yu, A.B.; Shen, Y. CFD-DEM Simulation of Raceway Formation in an Ironmaking Blast Furnace. *Powder Technology* 2017, *Vol. 314*, pp. 542-549.
12. Yeh, C.P.; Du, S.W.; Tsai, C.H.; Yang, R.J. Numerical Analysis of Flow and Combustion Behavior in Tuyere and Raceway of Blast Furnace Fueled with Pulverized Coal and Recycled Top Gas. *Energy* 2012, *Vol. 42*, pp. 233-240.
13. Babich, A.; Senk, D.; Gudenau, H. W. An Outline of the Process. In *Ironmaking*; Verlag Stahleisen GmbH, Dusseldorf, Germany, 2016, pp. 180-185.

14. Vuokila, A.; Mattila, O.; Keiski, R. L.; Muurinen, E. CFD Study on the Heavy Oil Lance Positioning in the Blast Furnace Tuyere to Improve Combustion. *ISIJ International* 2017, *Vol. 57*, pp. 1911-1920.

15. Austin, P.R.; Nogami, H.; Yagi, J. A Mathematical Model of Four Phase Motion and Heat Transfer in the Blast Furnace. *ISIJ International* 1997, *Vol. 37*, pp. 458–467.

16. Natsui, S.; Ueda, S.; Nogami, H.; Kano, J.; Inoue, R.; Ariyama, T. Analysis of Non-Uniform Gas Flow in Blast Furnace Based on DEM-CFD Combined Model. *Steel Research International* 2011, *Vol. 82*, pp. 964-971.

17. Kon, T.; Natsui, S.; Matsuhashi, S.; Ueda, S.; Inoue, R.; Ariyama, T. Influence of Cohesive Zone Thickness on Gas Flow in Blast Furnace Analyzed by DEM-CFD Model Considering Low Coke Operation. *Steel Research International* 2013, Vol. 84, pp. 1146-1156.

18. Majeski, A.; Runstedtler, A.; D'Alessio, J.; Macfadyen, N. Injection of Pulverized Coal and Natural Gas into Blast Furnaces for Iron-making: Lance Positioning and Design. *ISIJ International* **2015**, *Vol. 55*, pp. 1377-1383.

19. Dong, X.F.; Yu, A.B.; Chew, S.J.; Zulli, P.; Modeling of Blast Furnace with Layered Cohesive Zone. *Metallurgical and Materials Transactions B* 2010, *Vol. 41*, pp. 330-349.

20. Bool, L.E.; Damstedt, B.; Mocsari, J., "Oxygen Reforming of Tar and Methane in Biomass Derived Syngas", Proceedings of the 22nd Annual Energy, Utility, Environment Conference, San Diego, CA, U.S.A., Feb. 25-26, 2019, 8 pgs.

21. Beer, J. M.; Chigier, N. A. *Combustion Aerodynamics*; Applied Science Publishers, London, 1972.

22. Fu, D.; Zheng, D.; Zhou, C.Q.; D'Alessio, J.; Ferron, K.J.; Zhao, Y. Parametric Studies on PCI Performances. Proceedings of the ASME/JSME 2011 8th Thermal Engineering Joint Conference, Honolulu, Hawaii, United States, Paper no. AJTEC2011-44608, 2011.

23. Chen, Y.; Fu, D.; Zhou, C. Q.; Numerical Simulation of the Co-Injection of Natural Gas and Pulverized Coal in Blast Furnace. Proceedings of AISTech 2013, Pittsburgh, PA, U.S.A., May 6-9, 2013, pp. 573-580.

24. Silaen, A. K.; Okosun, T.; Chen, Y.; Wu, B.; Zhao, J.; Zhao, Y.; D'Alessio, J.; Capo, J.; Zhou, C.Q. Investigation of High Rate Natural Gas Injection through Various Lance Designs in a Blast Furnace. Proceedings of AISTech 2015, Cleveland, OH, U.S.A., May 4-7, 2015, pp. 1536-1549.

25. Okosun, T.; Street, S.; Chen, Y.; Zhao, J.; Wu, B.; Zhou, C.Q. Investigation of Co-Injection of Natural Gas and Pulverized Coal in a Blast Furnace. Proceedings of AISTech 2015, Cleveland, OH, U.S.A., May 4-7, 2015, pp. 1581-1594.

26. Okosun, T.; Street, S.J.; Zhao, J.; Wu, B.; Zhou, C.Q. Investigation of Dual Lance Designs for Pulverized Coal and Natural Gas Co-Injection. Proceedings of AISTech 2016, Pittsburgh, PA, U.S.A., May 16-19, 2016, pp. 581-594.

27. Okosun, T.; Street, S. J.; Zhao, J.; Wu, B.; Zhou, C.Q. Influence of Conveyance Methods for Pulverized Coal Injection in a Blast Furnace. *Ironmaking and Steelmaking* 2017, *Vol. 44*, pp. 513-525.

28. Okosun, T.; Liu, X.; Silaen, A.K.; Barker, D.; Dybzinksi, D.P.; Zhou, C.Q. Effects of Blast Furnace Auxiliary Fuel Injection Conditions and Design Parameters on Combustion Characteristics and Injection Lance Wear. Proceedings of AISTech 2017, Nashville, TN, U.S.A., May 8-11, 2017, 11 pgs.
29. Okosun, T.; Nielson, S.; D'Alessio, J.; Klaas, M.; Street, S.J.; Zhou, C.Q. Investigation of High-Rate and Pre-heated Natural Gas Injection in the Blast Furnace. Proceedings of AISTech 2019, Pittsburgh, PA, U.S.A., May 6-9, 2019, 15 pgs.
30. Okosun, T.; Silaen, A.K.; Zhou, C.Q. Review on Computational Modeling and Visualization of the Ironmaking Blast Furnace at Purdue University Northwest. *Steel Research International* **2019**, *Vol. 90*.
31. Fu, D. Numerical Simulation of Ironmaking Blast Furnace Shaft. Ph.D. Dissertation, Purdue University, West Lafayette, IN, U.S.A., May 2014.
32. Okosun, T. Numerical Simulation of Combustion in the Ironmaking Blast Furnace Raceway. Ph.D. Dissertation, Purdue University, West Lafayette, IN, U.S.A., May 2018.
33. Launder, B.; Spalding, D. *Lectures in Mathematical Models of Turbulence*. Academic Press: New York, NY, U.S.A., 1972.
34. Gu, M.; Zhang, M.; Selvarasu, N.K.C.; Zhao, Y.; Zhou, C.Q.; Numerical Analysis of Pulverized Coal Combustion inside Tuyere and Raceway. *Steel Research International* 2008, *Vol. 79*, pp. 17-24.
35. Gu, M.; Chen, G.; Zhang, M.; Huang, D.; Chaubal, P.; Zhou C.Q. Three-dimensional Simulation of the Pulverized Coal Combustion inside Blast Furnace Tuyere. *Applied Mathematical Modelling* 2010, *Vol 34*, pp. 3536-3546.
36. Huang, D.; Tian, F.; Chen, N.; Zhou, C.Q. A Comprehensive Simulation of the Raceway Formation and Combustions. Proceedings of AISTech 2009, St. Louis, MO, U.S.A., May 4-7, 2009.
37. Fu, D.; Huang, F.; Tian, F.; Zhou, C.Q. Burden Descending and Redistribution in a Blast Furnace. Proceedings of AISTech 2010, Pittsburgh, PA, U.S.A., May 3-6, 2010.
38. Zhou C. Q., *Minimization of Blast Furnace Fuel Rate by Optimizing Burden and Gas Distribution*. Final Technical Report to U.S. Department of Energy (DOE), 2012.
39. Fu, D.; Chen, Y.; Rahman, Md.T.; Zhou, C.Q. Prediction of the Cohesive Zone in a Blast Furnace. Proceedings of AISTech 2011, Indianapolis, IN, U.S.A., May 2-5, 2011.